LANGLEY GRANT
IN-39-CR
154660
75P.

AN EXPERIMENTAL AND ANALYTICAL EVALUATION OF A BIAXIAL TEST FOR DETERMINING SHEAR PROPERTIES OF COMPOSITE MATERIALS

by

John M. Kennedy[1]

and

Terry R. Barnett[2]

Department of Mechanical Engineering

Clemson University

July 1988

[1]Assistant Professor of Mechanical Engineering

[2]Graduate Student, Department of Mechanical Engineering

(NASA-CR-182928) AN EXPERIMENTAL AND ANALYTICAL EVALUATION OF A BIAXIAL TEST FOR DETERMINING SHEAR PROPERTIES OF COMPOSITE MATERIALS (Clemson Univ.) 75 p CSCL 20K

N88-27593

Unclas

G3/39 0154660

AN EXPERIMENTAL AND ANALYTICAL EVALUATION OF

A BIAXIAL TEST FOR DETERMINING SHEAR

PROPERTIES OF COMPOSITE MATERIALS

by

John M. Kennedy[1]

and

Terry R. Barnett[2]

Department of Mechanical Engineering

Clemson University

July 1988

[1]Assistant Professor of Mechanical Engineering

[2]Graduate Student, Department of Mechanical Engineering

ABSTRACT

The results of an experimental and analytical investigation of a biaxial tension/compression test for determining shear properties of composite materials are reported. Using finite element models of isotropic and orthotropic laminates, a specimen geometry was optimized. The optimized specimen has:

1. a large area of pure shear whose magnitude equals that of the applied stress,
2. small stress gradients around the boundary of the test section,
3. geometry that is independent of laminate orientation, and
4. a geometry that is easy to manufacture.

A kinematic fixture was designed to introduce an equal and opposite pair of forces into a specimen with a one inch square test section. Aluminum and several composite laminates with the optimized geometry and a configuration with large stress gradients were tested in the fixture. The specimens were instrumented with strain gages in the center of the test section for shear stiffness measurements. Pure shear strain was measured. The results from the experiments correlated well with finite element results. Failure of the specimens occurred through the center of the test section and appeared to have initiated at the high stress points. The results lead to the conclusion that the optimized specimen is suitable for determining shear modulus for composite materials. Further revisions to the specimen geometry are necessary if the method is to give shear strength data.

CHAPTER I

INTRODUCTION

Literature Review

The use of advanced composite materials for structures requiring high strength and stiffness with minimum weight, has dictated the need for determining the mechanical properties of these materials. However, mechanical properties such as tensile, compressive, and shear response can be extremely difficult and expensive to determine. The "ideal" test should have:

1. a specimen that is easy to fabricate,
2. a test fixture that can be used in most experimental laboratories,
3. the ability to give accurate and reproducible results, and
4. be inexpensive.

In particular, measurement of shear properties is especially difficult because of the problems in specifying a suitable specimen geometry and loading condition that results in a pure shear stress state of known magnitude. In the "ideal" shear specimen, the stress state in the entire test section would be uniform pure shear. In light of this, numerous test methods have been proposed for determining the shear response of advanced composite materials, but none of these methods has been adopted by the composite community as the "perfect shear test."

Lee and Munro (1) evaluated the primary in-plane shear test methods. Each method was rated according to its cost of fabrication, cost of testing, data reproducibility, and accuracy of experimental results.

They concluded that the top three shear test methods were the Iosipescu shear test, 45° off-axis tensile test, and the 10° off-axis tensile test.

The Iosipescu test, rated as the best method by Lee and Munro, is widely used because of simple specimen geometry, and because shear property measurements correlated very well with torsion of thin-walled tubes. (Torsion of a thin-walled tube provides a means of directly introducing a shear load and is usually considered the most accurate in measurement of shear properties.) However, Pindera, et. al (2), showed that the stress state in the test section of the Iosipescu specimen was nonuniform. The results indicated that the discrepancy between the experimentally measured shear modulus and predicted shear modulus was due to this nonuniformity. Pindera proposed that correction factors obtained from finite element analysis could be introduced. It was also reported by Lee and Munro that in the case of composites, the stress distribution deviates from ideal conditions and may be dependent on laminate configuration. Also, there is a significant stress concentration at the root of the notch in unidirectional laminates. Although the Iosipescu specimen was rated best, it did not receive a perfect score.

According to Lee and Munro, the method with the lowest rating and the method that will be studied herein, was the cross-beam specimen. The cross-beam specimen is made by bonding two thin sheets of composite on each side of a core, usually honeycomb, to form a sandwich panel. As shown in Figure 1, the cross-beam is loaded in multiaxial bending, which produces a biaxial state of tension and compression in the test section. Simple beam theory predicts a state of pure shear at 45° to the loading directions (Figure 2) with the magnitude of the shear stress equal to

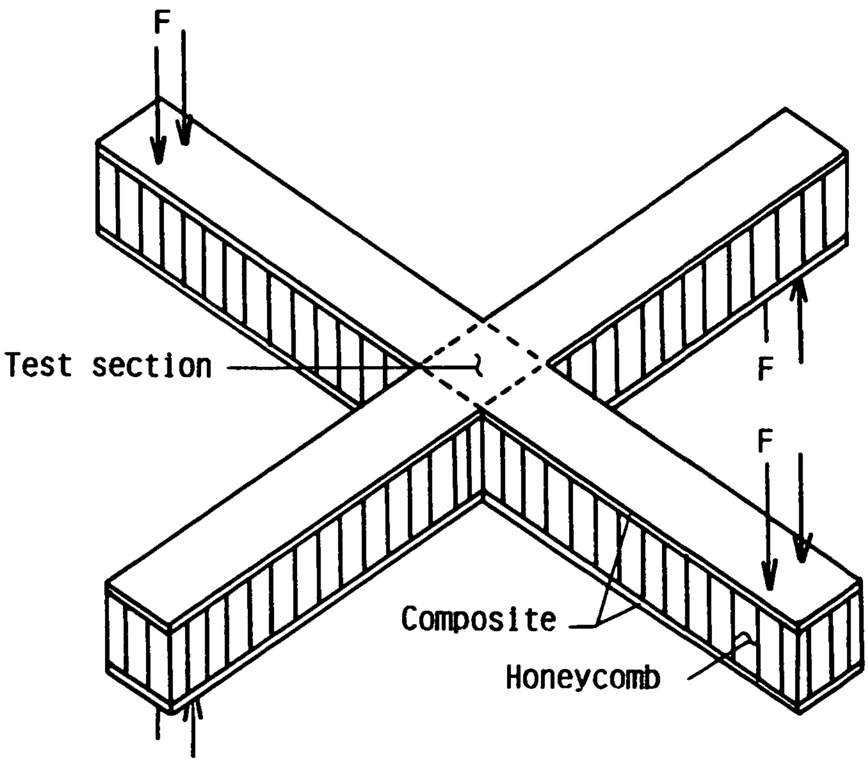

Figure 1. The Cross-Beam Sandwich Specimen

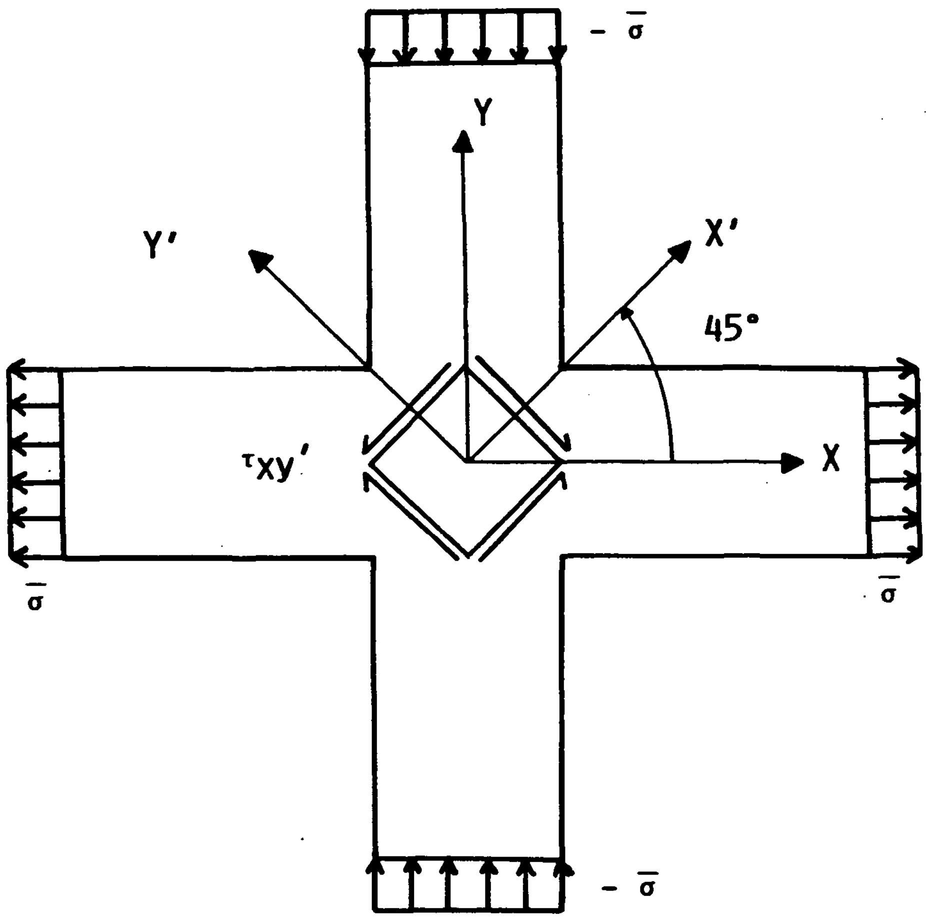

Figure 2. Pure Shear Loading as a Result of Biaxial Tension/Compression

that of the bending stress. The cross-beam received the lowest score due to:

1. the size of the specimen,
2. an unusual testing apparatus,
3. long set up and actual testing time,
4. significant normal stresses in the corner of the test section,
5. low shear strength measurements compared to torsion of a thin-walled tube, and
6. core indluences.

Several studies have been conducted on the cross-beam. Finite element analysis of the $[\pm 45]_s$ laminate by Bergner (3) predicted that the stress distribution in the center of the test section of the cross-beam was uniform pure shear, but that the ratio of the shear stress in the center of the test section to the applied stress, τ_{xy}'/σ, was greater than 1.0. Unlike the $[\pm 45]_s$ laminate the magnitude of the shear stress in the center of the test section of the $[0/90]_s$ was very close to 1.0, which shows that the magnitude of the shear stress in the center of the cross-beam is dependent on laminate properties. A value of τ_{xy}'/σ not equal to 1.0 indicates the shear stress in the center of the test section is less or greater than the applied stress; therefore, an incorrect shear modulus will be measured if it is assumed that the magnitude of the applied stress equals that of the shear stress. The condition of τ_{xy}'/σ not equal to 1.0 does not pose a problem if this value can be obtained from an analytical study such as finite element analysis. However, this is a disadvantage for an experimental method since a numerical analysis will have to be conducted for every different material. The "ideal shear test" should have a specimen such that the magnitude of the stress in the

test section is a known function of the applied stress and independent of laminate properties.

For both the $[0/90]_s$ and $[\pm 45]_s$ laminates, Bergner found severe stress gradients in the corners of the test section. From this he concluded that failure of the specimen may be premature and in mode different from pure shear. So, it is doubtful that the cross-beam will give accurate shear strength data.

Duggan, McGrath, and Murphy (4) compared finite element results from the cross-beam to the similarly loaded slotted tensile specimen of Figure 3. Their results showed that the region of pure shear in the slotted tensile coupon was larger than that of the cross-beam. Also, stress concentrations at the root of the slot were not as severe as those in the sharp corners of the cross-beam. For the $[\pm 45]_s$ laminate, the slotted tensile coupon was within 2 percent of the applied shear stress, while the cross-beam was 13 to 20 percent high. For the $[0/90]_s$ laminate, the cross-beam and the slotted tensile coupon gave only small deviations from the applied stress.

Monch and Galster (5) used photoelastic stress analysis to show that effects of stress concentrations in the corners of a specimen under uniform biaxial tension could be significantly reduced by slitting the legs of the specimen into strips, as shown in Figure 4. Their results also showed that a region of uniform stress covered most of the test section. Cridland and Wood (6) also used photoelastic stress analysis to confirm these results.

Petit (7) compared experimental results of graphite/epoxy and boron/epoxy laminates from the cross-beam specimen and the 45° off-axis tensile test. He found excellent agreement along the initial portions

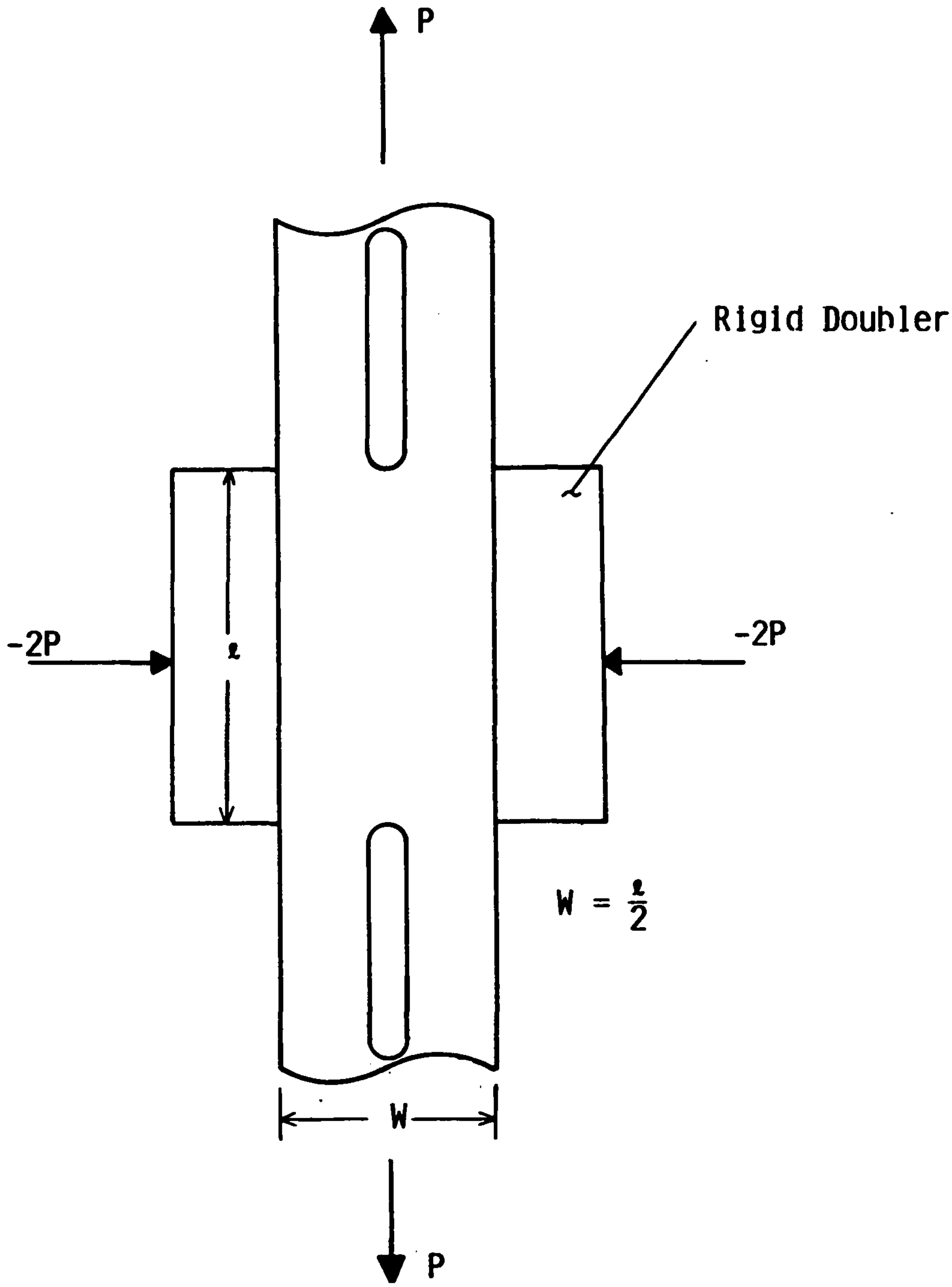

Figure 3. The Slotted Tensile Specimen

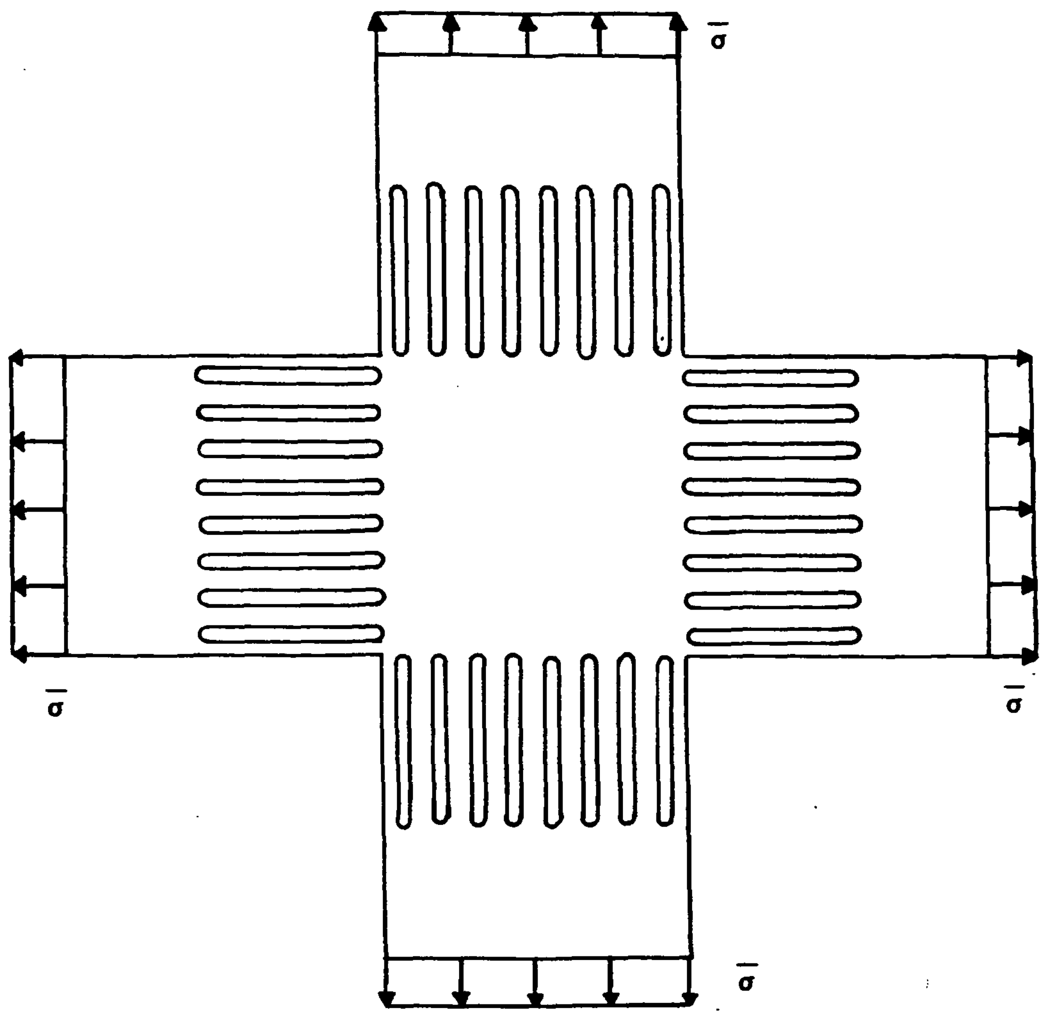

Figure 4. The Cruciform Tensile Specimen with Multiple Slits

of the shear stress-strain curves. However, at higher strains, the curves began to deviate from one another, with the cross-beam specimen having a significantly higher failure stress.

Objective

Researchers have analytically predicted and experimentally shown that the shear stress in the test section of the cross-beam is pure and uniform, but its magnitude is greater than the applied stress due to stress concentrations and core effects (3). Also, a testing apparatus that induces bending moments into the specimen is difficult to use in most experimental laboratories. Clearly, there are several options to improve this method.

The objective of this study was to investigate the coreless cross-beam specimen, i.e., the cruciform specimen (Figure 5), as a possible test method for measuring shear response of composite materials. This configuration has the advantage of direct application of tensile and compressive stresses with a simple kinematic type fixture (Figure 6). It can be used in a standard universal testing machine. The specimen is a flat coupon so there can be no influence of a core, as in the cross-beam. The advantage of being a planar specimen will also make its fabrication very easy.

Herein, the effect of geometry on the stress state in the test section of the cruciform specimen was examined using the finite element method. An optimized specimen geometry was determined and an experimental program was conducted to verify the finite element analysis.

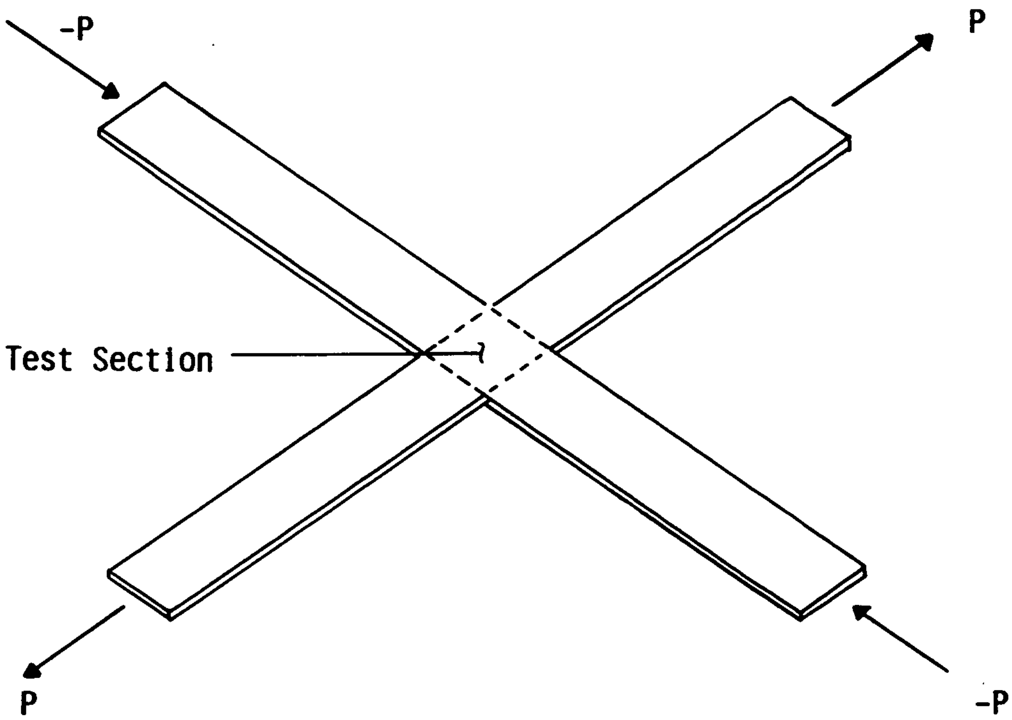

Figure 5. The Cruciform Specimen

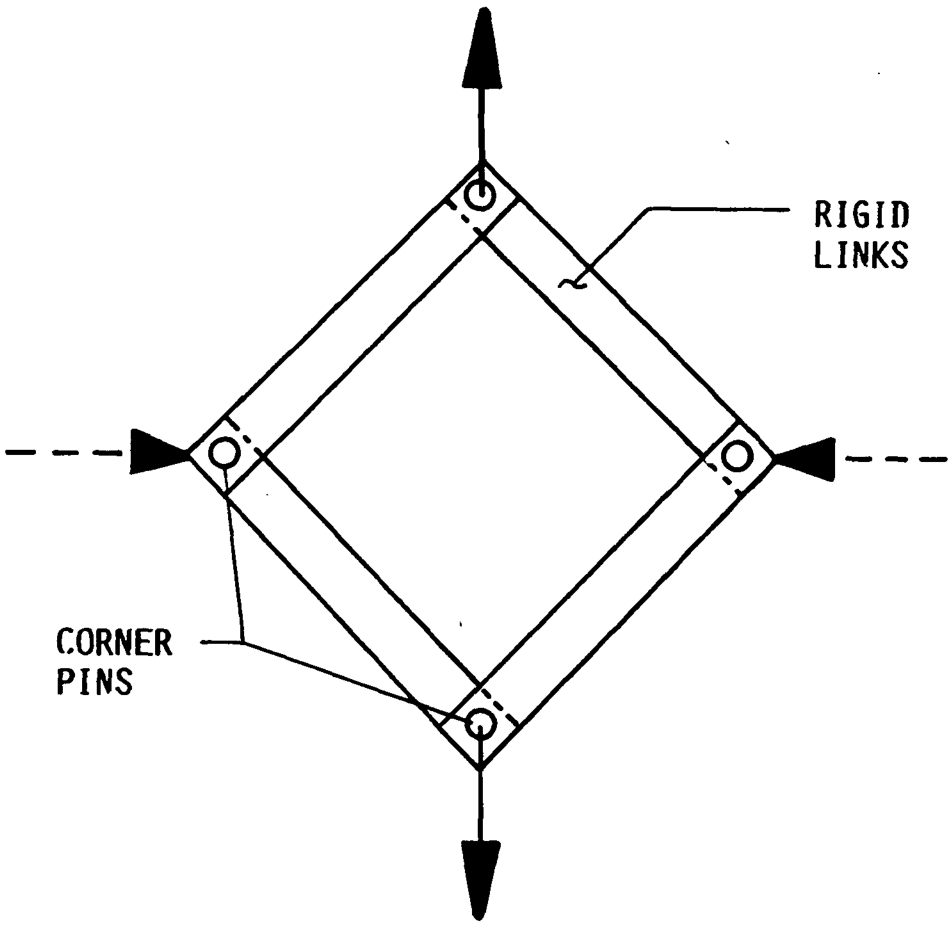

Figure 6. Picture Frame Test Fixture

CHAPTER II

FINITE ELEMENT ANALYSIS

Bergner predicted that the shear stress in the test section of the cross-beam was higher than the applied stress. It was suspected that these high shear stresses were a result of the stress concentrations in the geometrically discontinuous corners. Finite element analysis was employed to determine the effect of geometry on the stress state of the cruciform specimen. Isotropic, $[0/90]_s$ graphite/epoxy, and $[\pm 45]_s$ graphite/epoxy laminates were analyzed. The three geometrical configurations investigated were: (1) the cruciform specimen with sharp corners, (2) the slitted cruciform specimen, and (3) the cruciform specimen with corner radii. Stress contour plots, normalized with respect to the applied stress σ, are given in the following sections.

Because the pure shear stress state acts on an element oriented 45° to the applied biaxial tension/compression load, the $[0/90]_s$ laminate (fibers at 0° and 90° to the loading direction of the fixture) gives the shear response of $[\pm 45]_s$ laminates. Likewise, the $[\pm 45]_s$ laminate (fibers at ±45° to the loading direction) gives the shear response of $[0/90]_s$ laminates. Because each laminae is in a state of pure shear in $[0/90]_s$ type laminates, the measured shear modulus is G_{12}.

Finite Element Models

The finite element code used during the course of the research was ANSYS. The models used in the elastic finite element analysis are shown in Figure 7. Each model was made up of two-dimensional quadrilateral and triangular, isoparametric plate elements. Isotropic and orthotropic

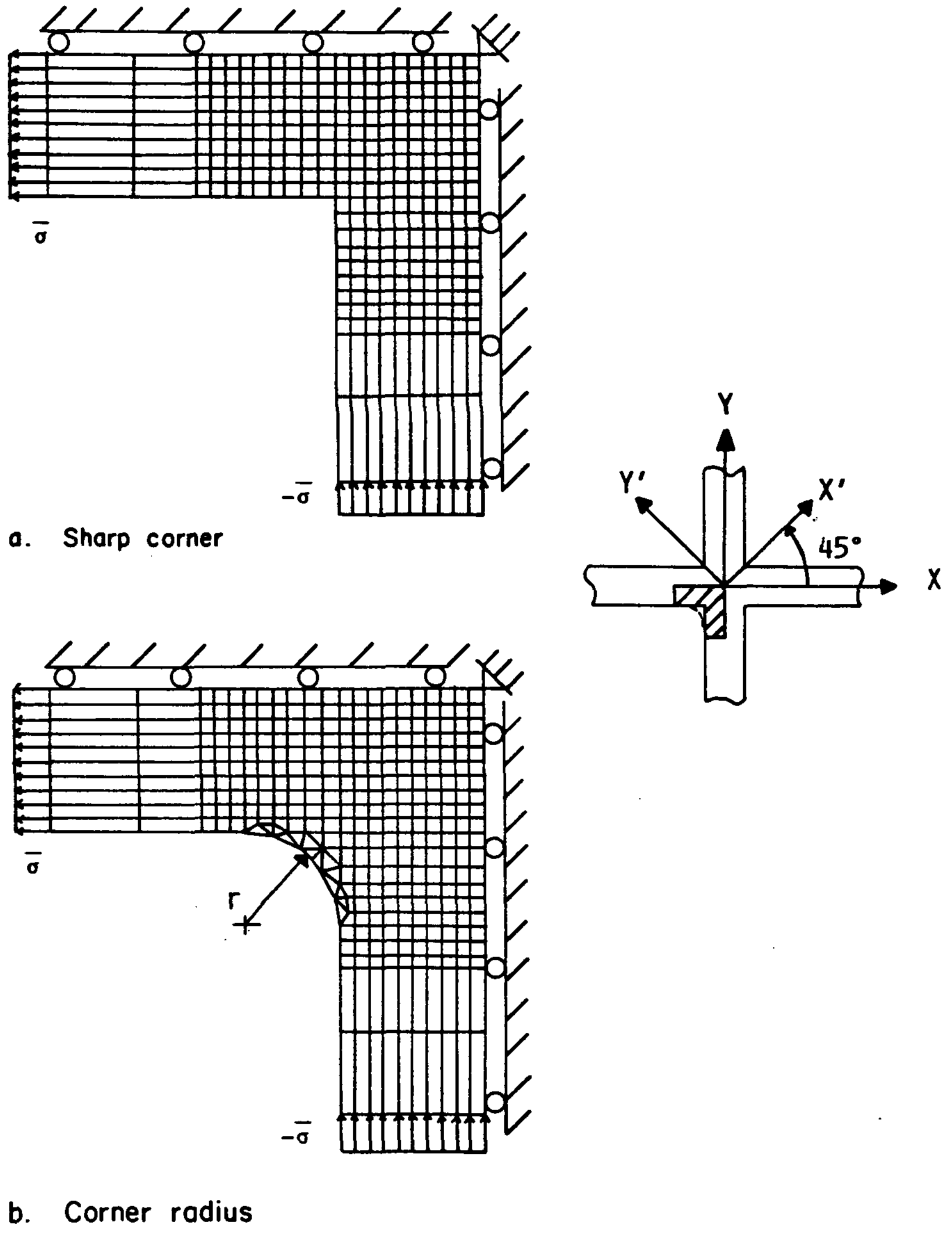

Figure 7. Finite Element Models of the Cruciform Specimen

specimens in a plane stress state were modeled. The material properties E_x, E_y, ν_{xy}, and G_{xy} were obtained from a laminate analysis program and used as input in the finite element code (8). The lamina properties used were those of a typical graphite/epoxy lamina.

A typical model for a specimen with sharp corners had approximately 363 nodes and 340 elements (Figure 7a), while a specimen with corner radii had 368 nodes and 355 elements (Figure 7b). Because of symmetrical geometry and loading, a model of only one quarter of the specimen was required. Along symmetry lines, displacement boundary conditions were enforced by imposing zero vertical displacements along the y-axis and zero lateral displacement along the x-axis. Loading conditions were simulated by the direct application of tensile and compressive stresses along the edges of the specimen. Because the models used only plate elements, there was no provision to determine interlaminar stresses along boundaries.

Results

The Cruciform Specimen with Sharp Corners

As mentioned, Bergner (1) conducted a comprehensive finite element analysis of the cross-beam specimen. He modeled both the composite and core to study the effects of core stiffness. The models used in this investigation were similar and the results obtained correlated very well for his cases of the $[0/90]_s$ and $[\pm45]_s$ laminates with flexible core material.

Isotropic Material

Figures 8-10 show the normalized τ_{xy}', σ_x', and σ_y' stress distributions for an isotropic material or a quasi-isotropic composite laminate. There was a region of pure shear in the center of the test section that

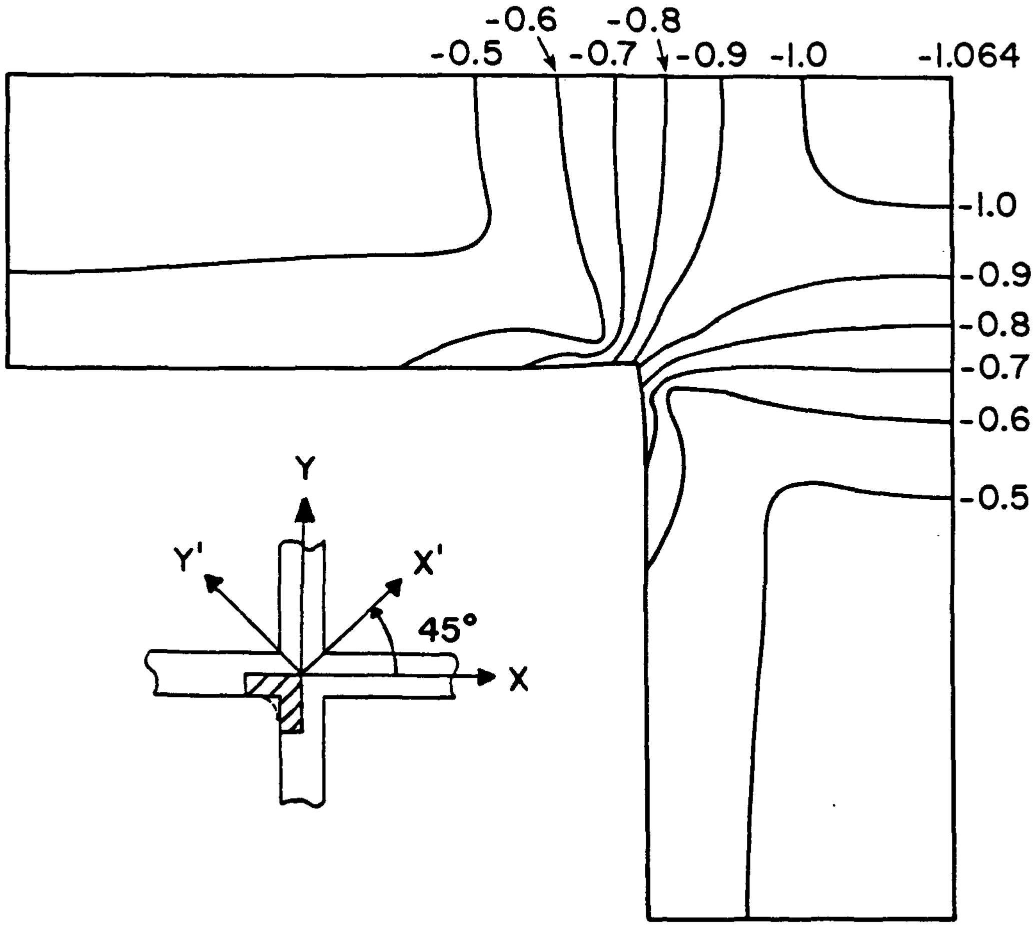

Figure 8. Normalized τ_{xy}' Contours for an Isotropic Cruciform Specimen with Sharp Corners

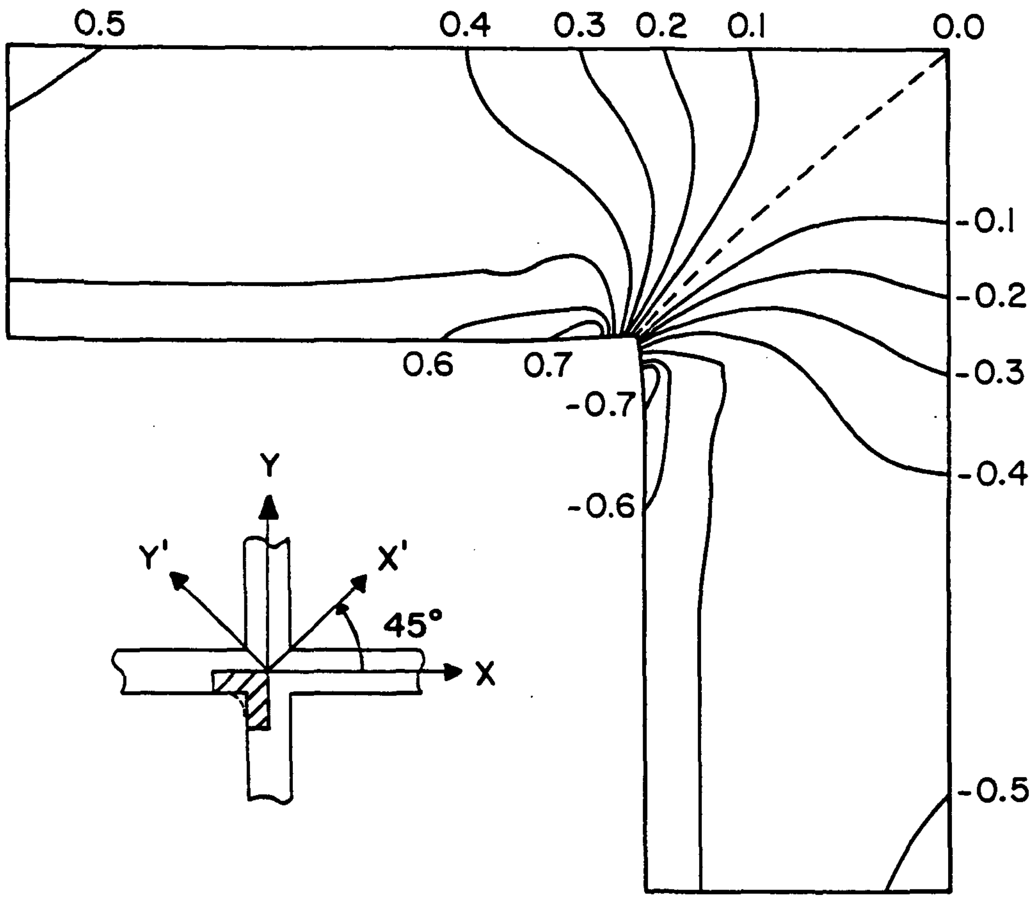

Figure 9. Normalized σ_x' Contours for an Isotropic Cruciform Specimen with Sharp Corners

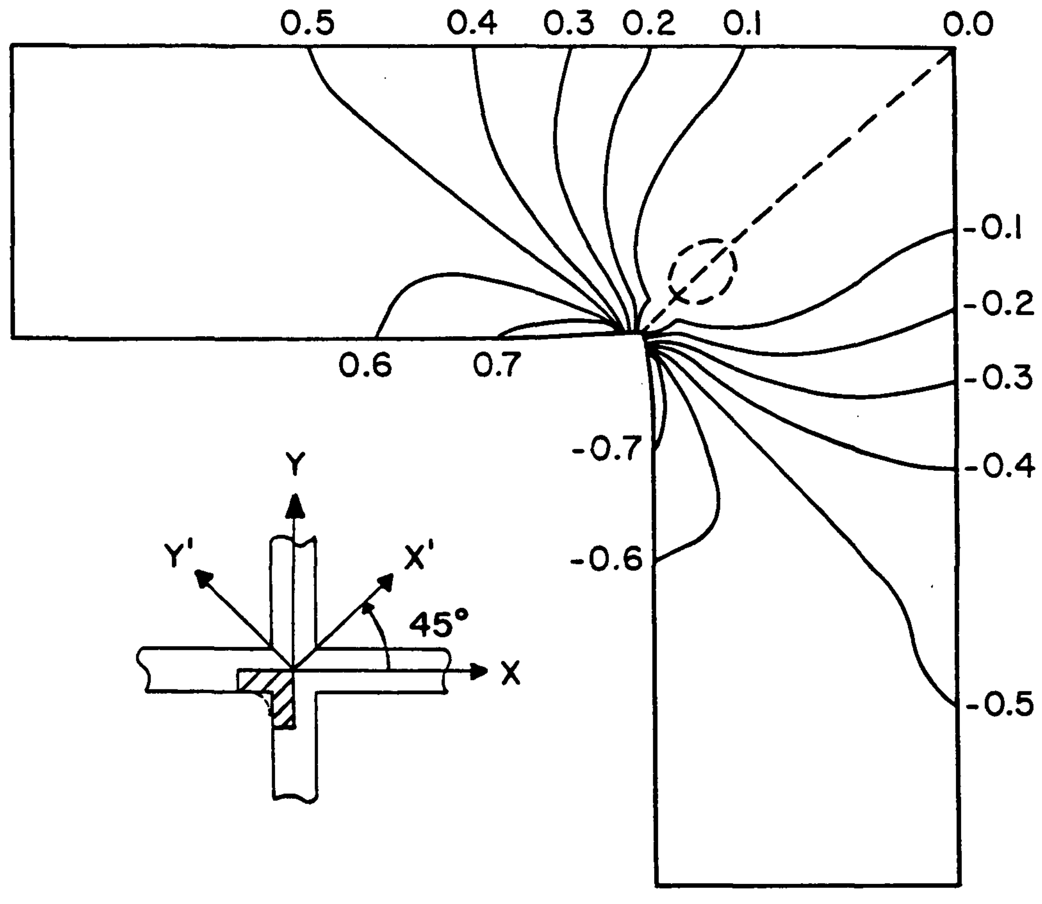

Figure 10. Normalized σ_y' Contours for an Isotropic Cruciform Specimen with Sharp Corners

was sufficiently large for experimental strain measurements. However, because the test section was only one inch square, the stress concentration in the corner effected the stress state in the center of the specimen. The magnitude of τ_{xy}'/σ in the center of the test section was 1.064, which showed the stress in the center of the test section was 6.4 percent higher than the applied stress, and measurement of shear modulus based only on applied stress will be low, or it must be corrected using results from an analytical study such as finite element analysis. If the test section were larger, the shear stress would be closer to the applied shear stress.

$[0/90]_s$ Laminate

Figures 11-13 show the results for the $[0/90]_s$ laminate. As in the isotropic case, the $[0/90]_s$ laminate had a region of pure shear in the test section, with a value of τ_{xy}'/σ equal to 1.024. The stress in the test section was 2.4 percent higher than the applied stress, and measurement of shear modulus based on applied stress would be only slightly low.

$[\pm45]_s$ Laminate

Figures 14-16 show the results for the $[\pm45]_s$ laminate. As in the previous cases, the $[\pm45]_s$ laminate had a region of pure shear in the center of the test section. However, the effect of the stress concentration in the corner was more severe. The value of τ_{xy}'/σ in the center of the section was 1.133, and measurment of stiffness based on applied stress would be significantly low.

From the results obtained for the three cases, it was clear that an accurate shear modulus cannot be experimentally determined if the

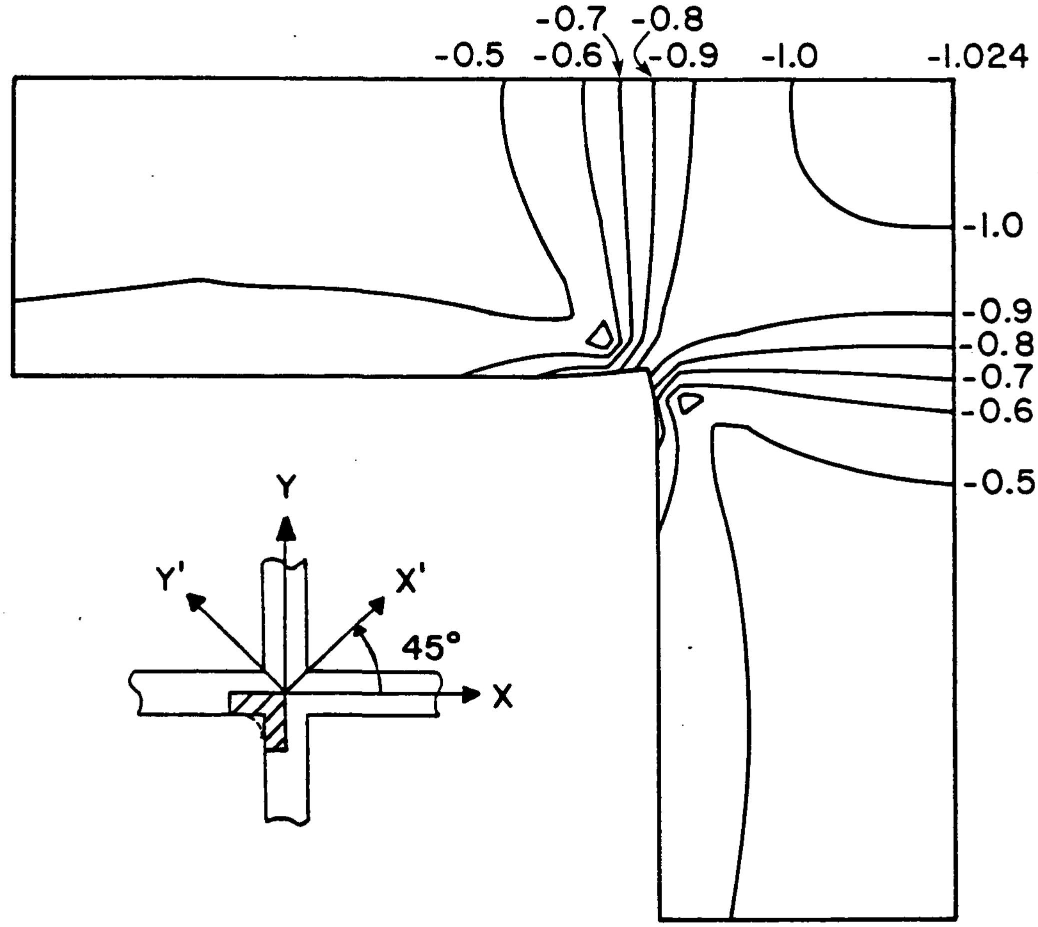

Figure 11. Normalized τ_{xy}' Contours for a $[0/90]_s$ Cruciform Specimen with Sharp Corners

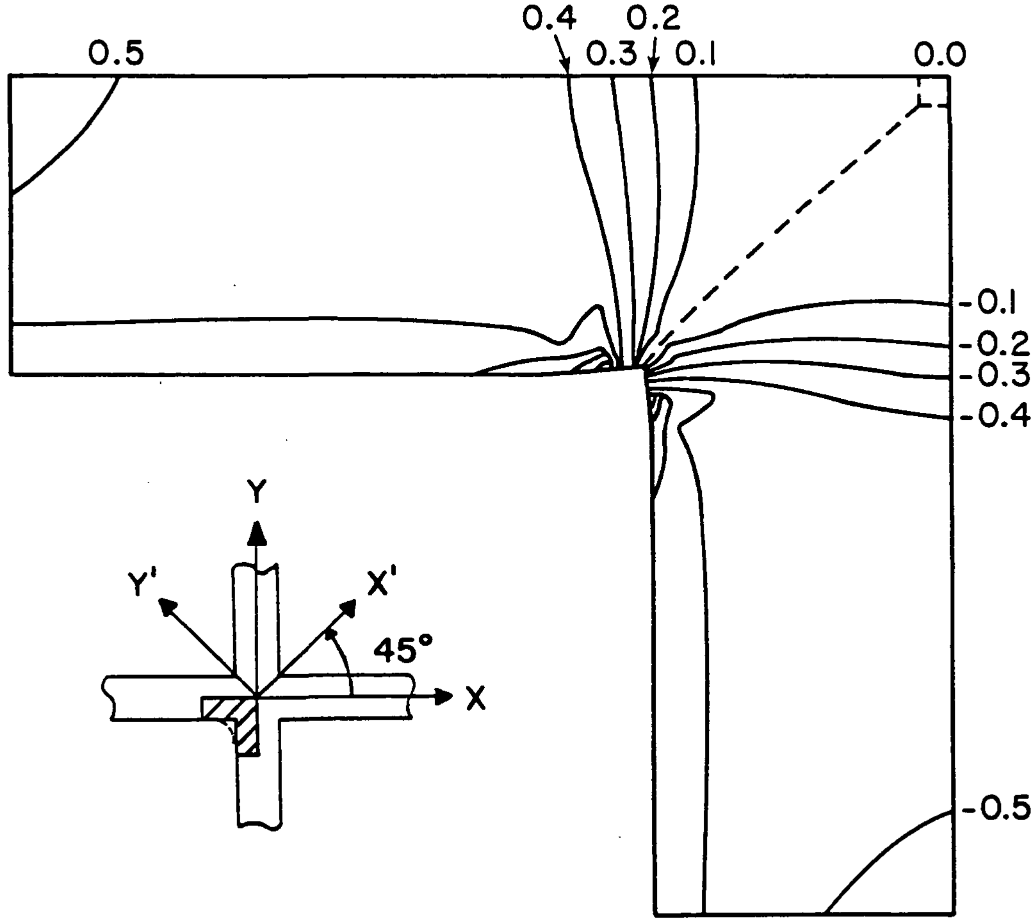

Figure 12. Normalized $\sigma_x{}'$ Contours for a $[0/90]_s$ Cruciform Specimen with Sharp Corners

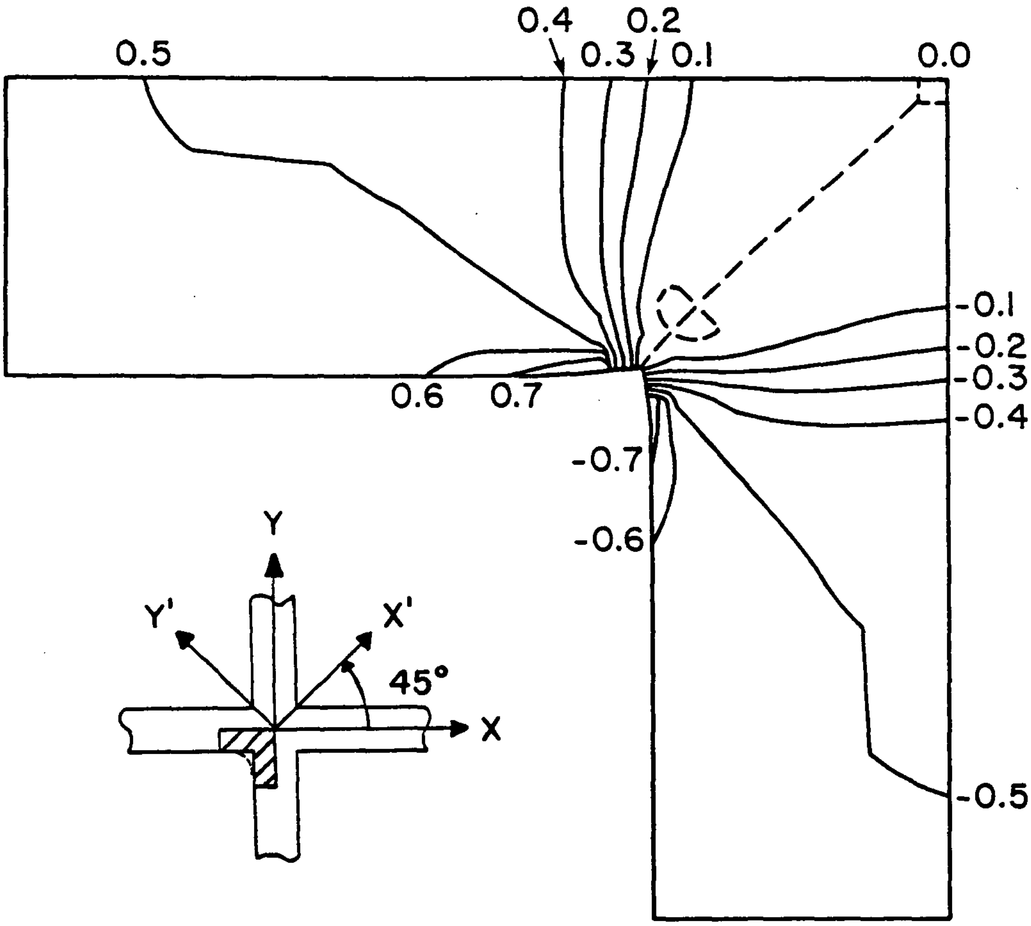

Figure 13. Normalized σ_y' Contours for a $[0/90]_s$ Cruciform Specimen with Sharp Corners

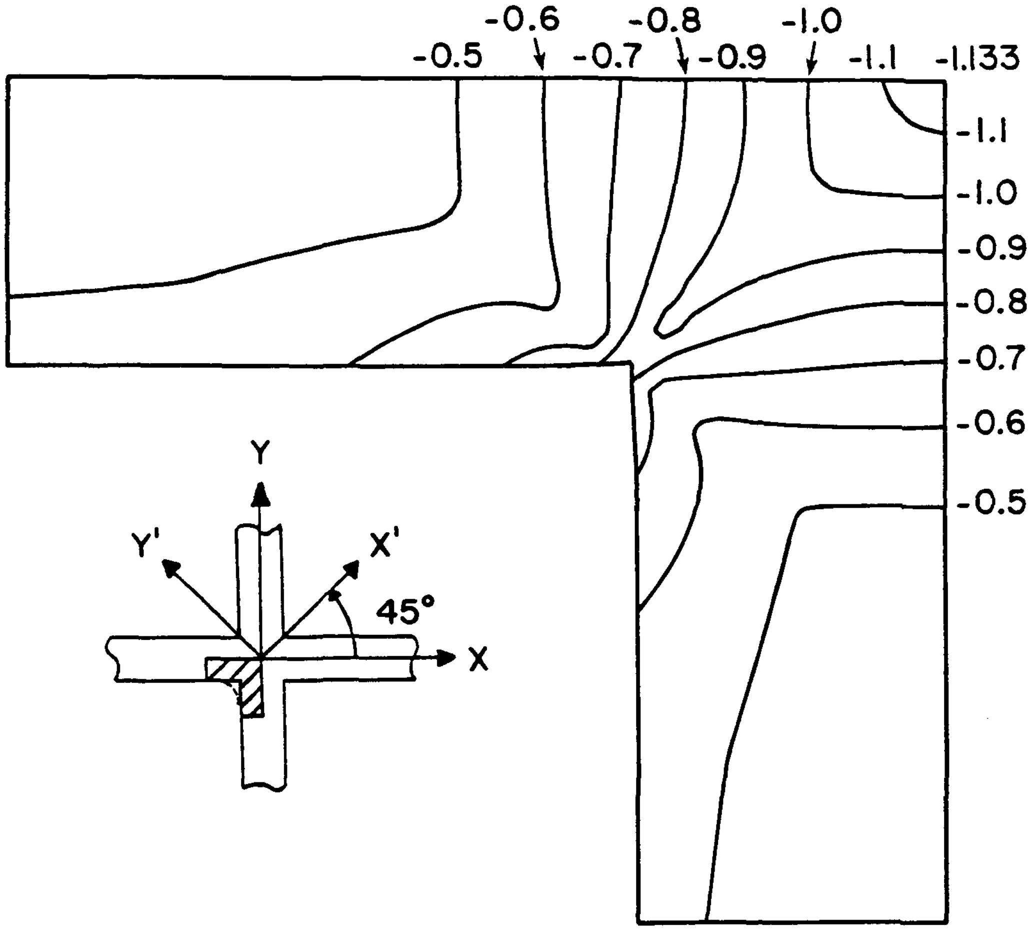

Figure 14. Normalized τ_{xy}' Contours for a $[\pm 45]_s$ Cruciform Specimen with Sharp Corners

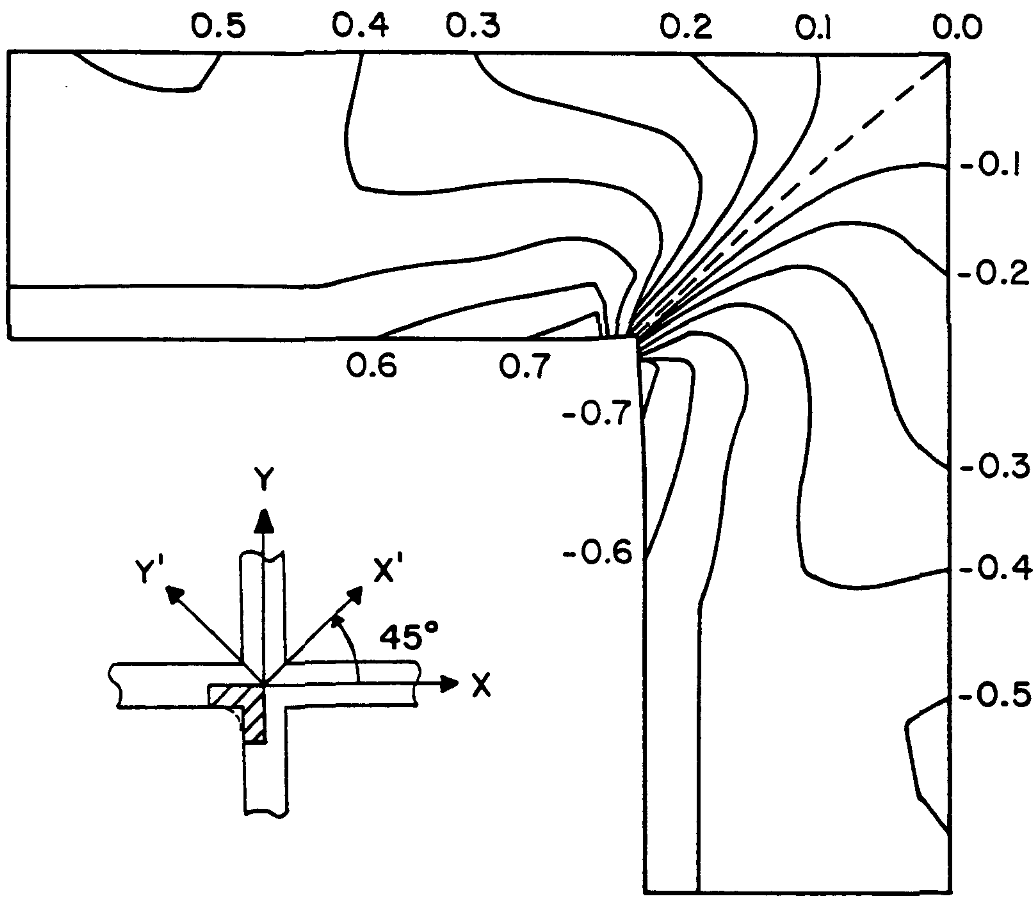

Figure 15. Normalized $\sigma_x{}'$ Contours for a $[\pm 45]_s$ Cruciform Specimen with Sharp Corners

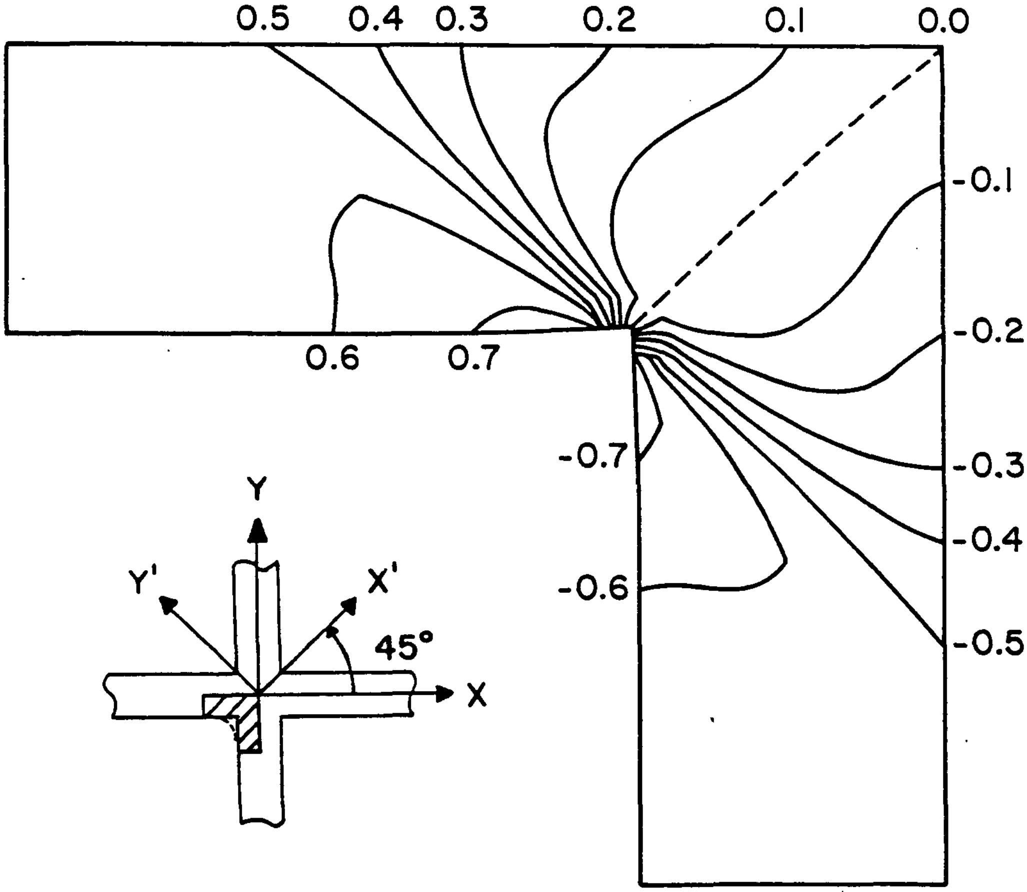

Figure 16. Normalized $\sigma_y{}'$ Contours for a $[\pm 45]_s$ Cruciform Specimen with Sharp Corners

magnitude of the applied stress is taken to be equal to the shear stress in the center of the test section. Because the center of the test section was in close proximity to the stress concentrations in the corners, the shear stress in the center of the test section was elevated. The effects of stress concentrations on the stress state in the center of the test section could be reduced by using a larger test section. However, buckling instabilities could become a factor. A larger testing fixture would be required as well as more material to fabricate the specimens. For smaller test sections, the effect of the concentrations on the stress in the test section would become even more prevalent.

Nodal stresses obtained from the finite element analysis were used in a Tsai-Wu failure analysis program. The program predicted the point in the specimen where failure would initiate. For the three cases studied, Tsai-Wu predicted that failure would initiate in the corner of the test section. It was concluded that measurement of failure strength with this geometry was doubtful.

The Slitted Cruciform Specimen

As previously discussed, Monch and Galster (5) showed that the effects of stress concentrations in the corners of a cruciform tensile specimen could be reduced by slitting the legs of the specimen into narrow strips. These slits allowed the regions just outside the test section to displace freely due to the biaxial load. This removes a constraint on the test section. Their results also showed that a uniform stress state existed over most of the test section.

Based on these results, it was hypothesized that a slitted specimen could be developed which gave a pure shear stress state. To study this specimen, the finite element model of Figure 7a was modified by deleting

selected elements along the boundary of the test section. The stress state in the test section varied with the number of slits, length of the slits, width of the slits, etc. Many configurations were studied. Only the results for an isotropic material and one configuration are presented.

Figures 17-19 confirmed that the effect of stress concentrations on the stress state in the test section was reduced and the stress state in the test section of the slitted cruciform was essentially uniform pure shear. The value of τ_{xy}'/σ in the center of the section could be made to be exactly 1.0 by further revisions to the slit geometry.

Although the stress state was pure shear over a large portion of the test section, the stress gradients in the regions between and around the slits were very high. All normalized components of stress in the corner of the specimen, as well as between the slits, were equal to or exceeded 1.0. Based on the magnitude of these stresses and the Tsai-Wu results from the previous section, failure would probably initiate near the slits. Also the specimen may buckle at the slits before a failure load can be reached. In the case of composite materials, anisotropy may influence the length, width, position, and number of slits needed to provide a uniform shear stress field. A more detailed parametric study could be conducted to determine the influence of these factors on the stress state in the specimen, but the impracticality of the design did not warrant such a study.

The Cruciform Specimen with Corner Radius

The results from previous sections predicted that the shear stress in the center of the test section was greater than the applied shear stress and that there were severe stress gradients at the corners and along the boundaries of the test section. Based on these results, sharp

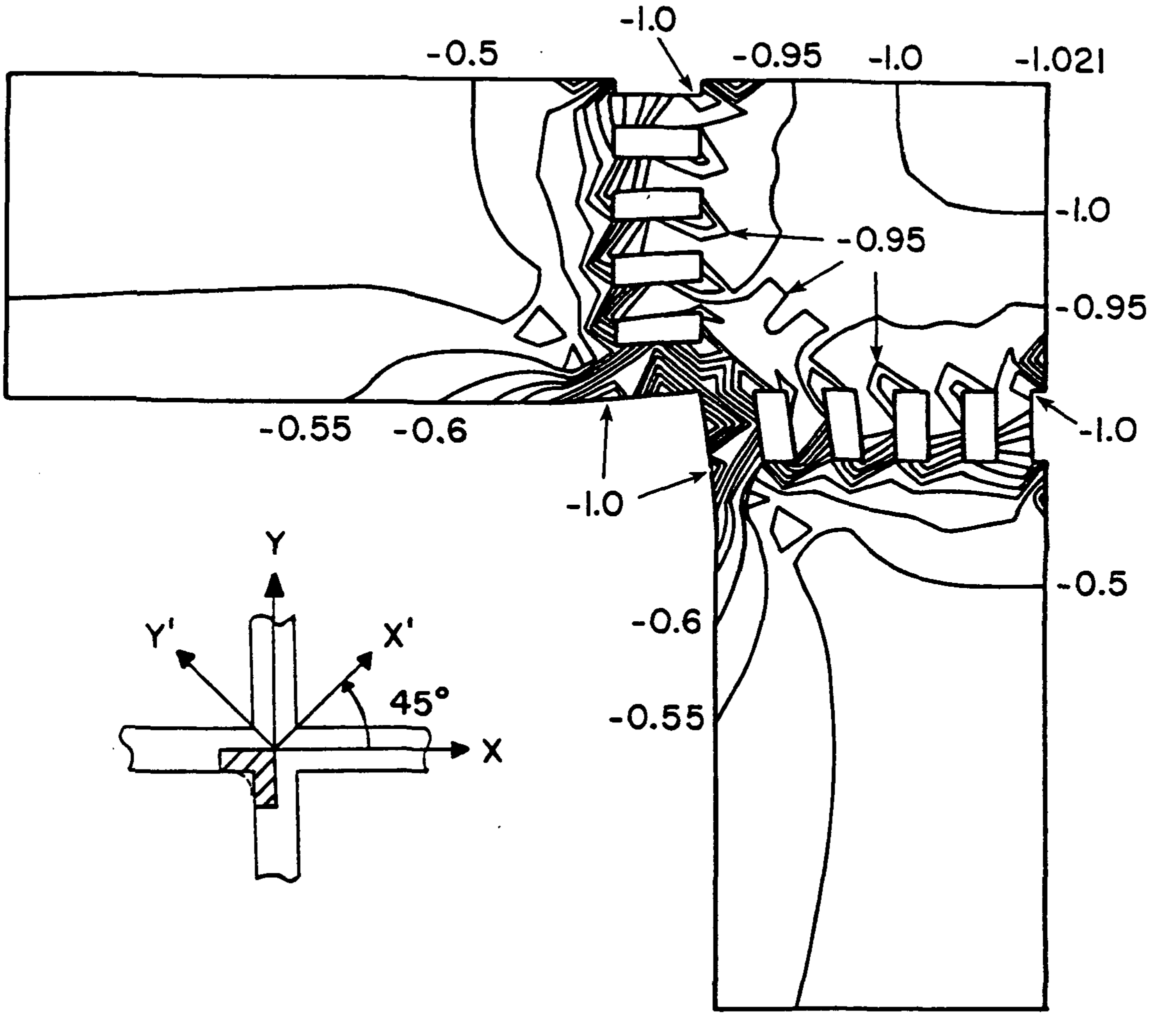

Figure 17. Normalized τ_{xy}' Contours for an Isotropic Cruciform Specimen with Slits

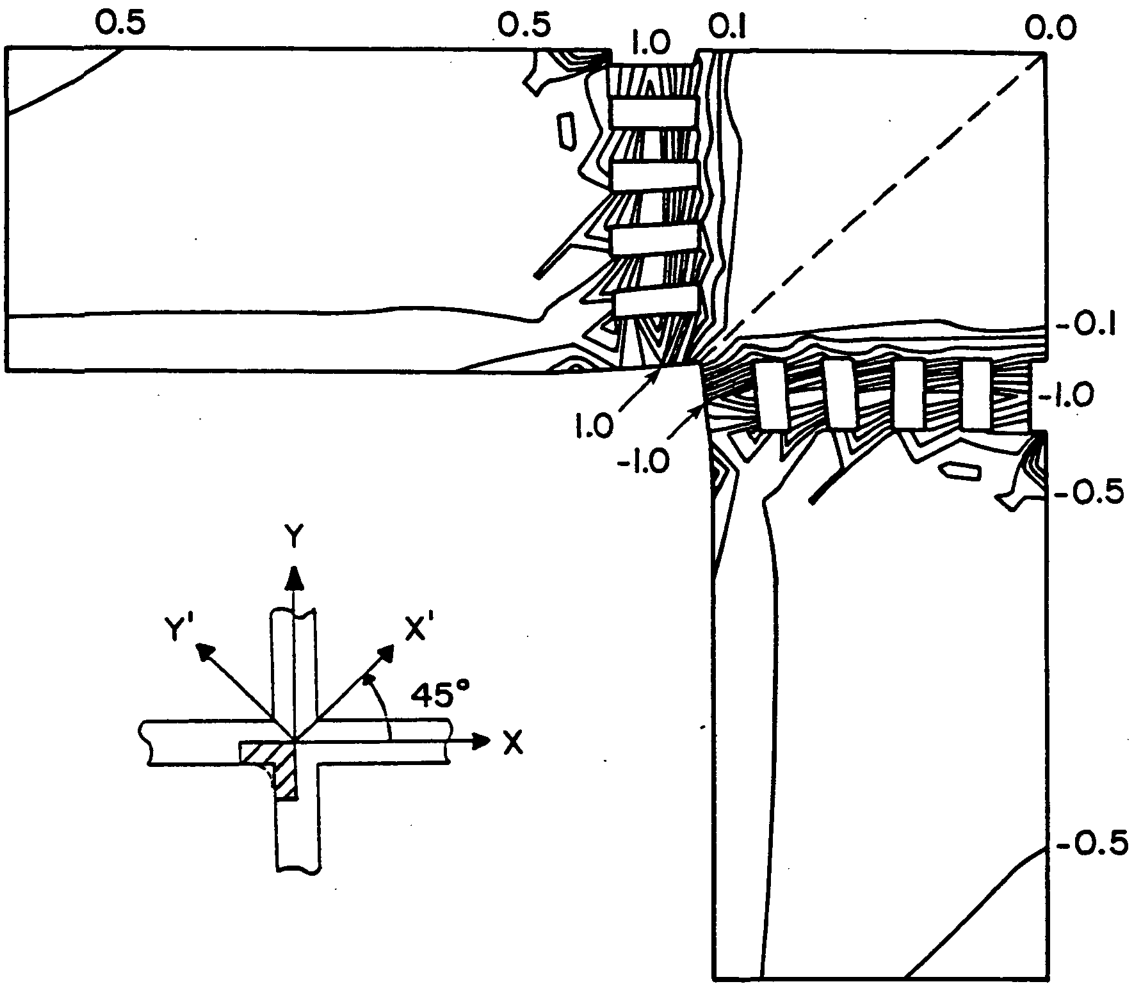

Figure 18. Normalized $\sigma_x{}'$ Contours for an Isotropic Cruciform Specimen with Slits

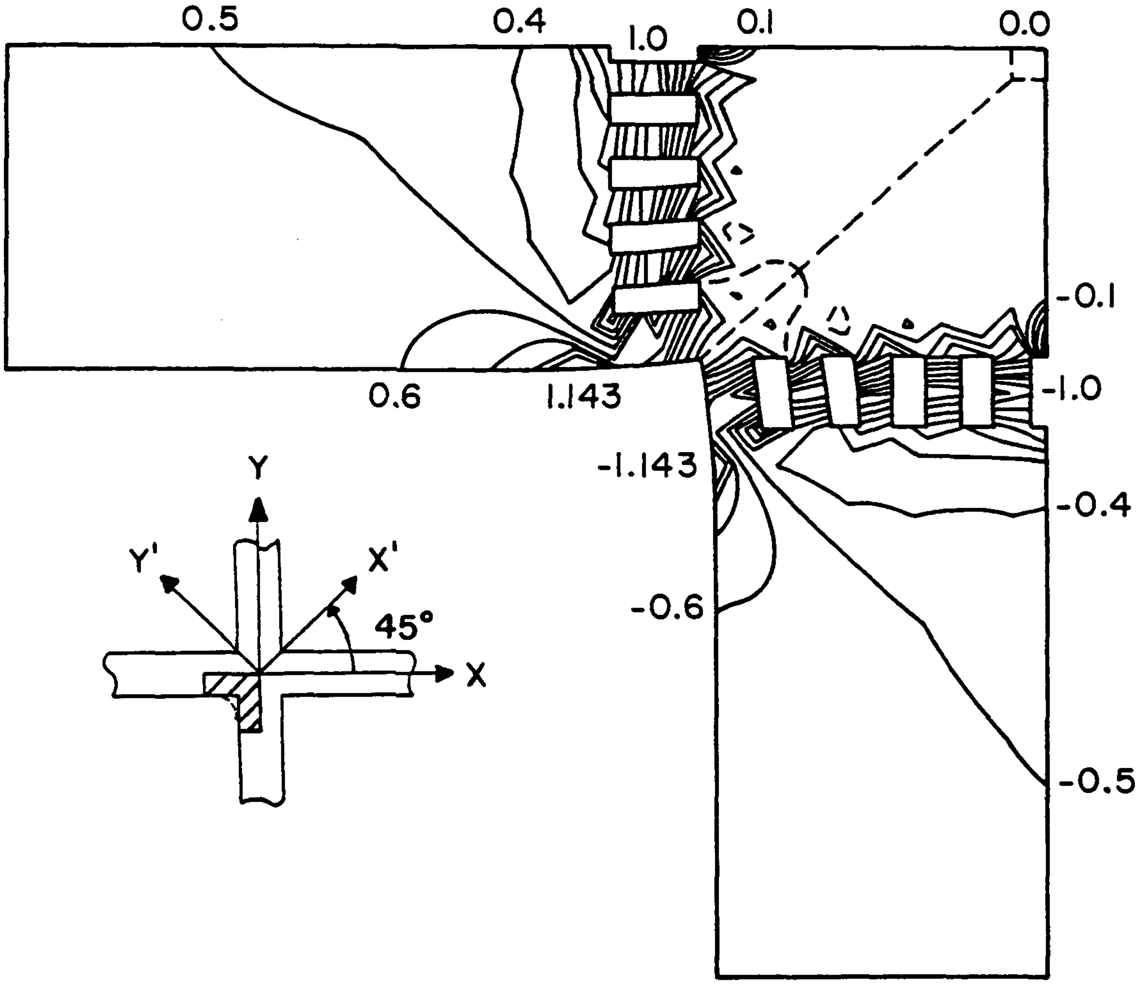

Figure 19. Normalized σ_{y}' Contours for an Isotropic Cruciform Specimen with Slits

corners were changed to large radii. This addition of material allows more load to be transferred to the legs of the specimen outside the test section, which should lower the shear stress in the center of the test section as well as the stress gradients. The finite element model of Figure 7b was used in this analysis.

The first step of the finite element analysis involved determining a corner radius which would give a value of τ_{xy}'/σ in the center of the test section equal (or very close) to 1.0 for each material type. The second step involved evaluating each material at that particular radius.

Specimens with 0.25, 0.33, and 0.50 inch corner radii were studied. As shown in Figure 20, τ_{xy}'/σ for each laminate converged to 1.0 between a corner radius of 0.30 and 0.40 inches. From the figure, a radius of approximately 0.35 inches gave a value of τ_{xy}'/σ less than 1.02. The results for the specimen with 0.33 inch corner radii are given below.

Isotropic Material

Figures 21-23 show the results for the isotropic material. There was a region of pure shear in the center of the specimen that was sufficiently large for experimental strain measurements. The magnitude of τ_{xy}'/σ in the the center of the test section was equal to 1.01, which show the applied stress was within 1.0 percent of the stress in the center of the test section and calculation of shear modulus based on applied stress should be very accurate. The severe stress gradients observed with the previous two geometries have been distributed along the arc of the radius; consequently, their effect on the stress distribution in the center of the test section was minimal.

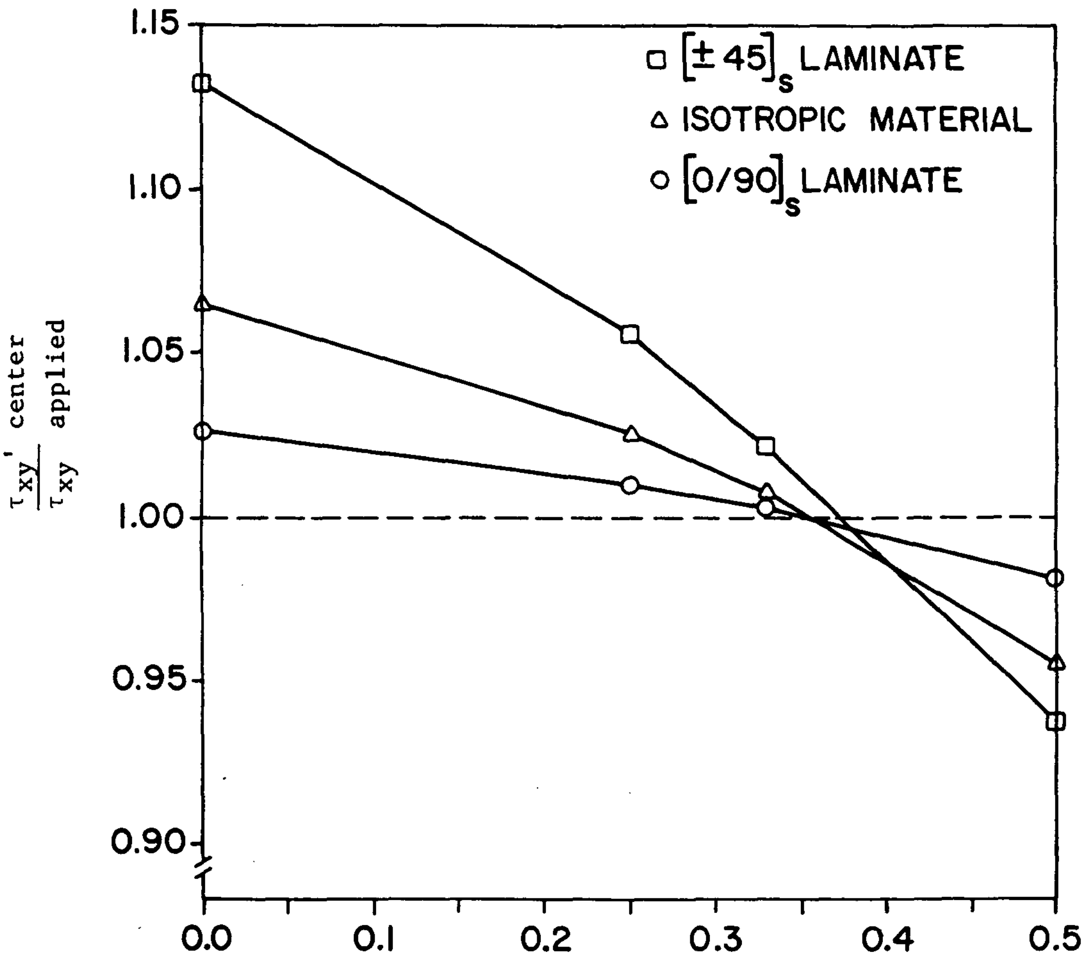

Figure 20. Variation of Shear Stress in the Center of the Test Section with Corner Radius

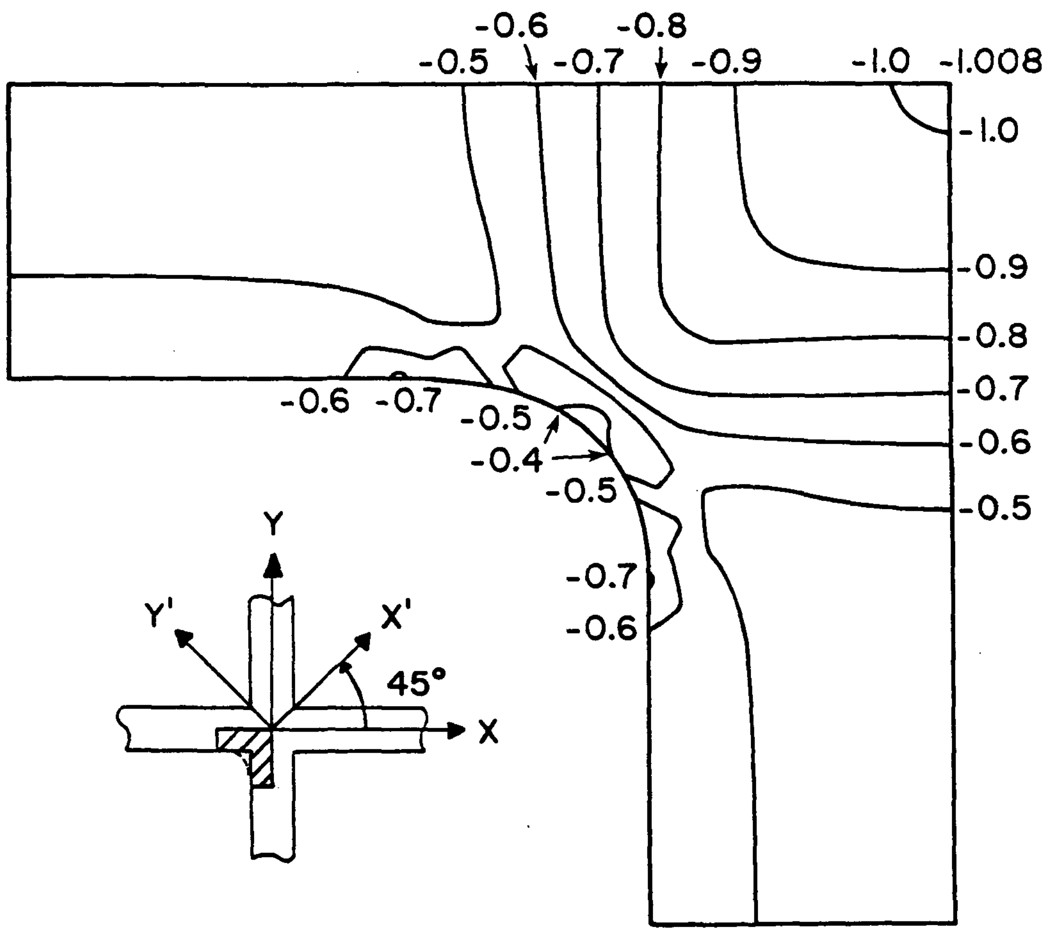

Figure 21. Normalized τ_{xy}' Contours for an Isotropic Cruciform Specimen with 0.33 Inch Corner Radii

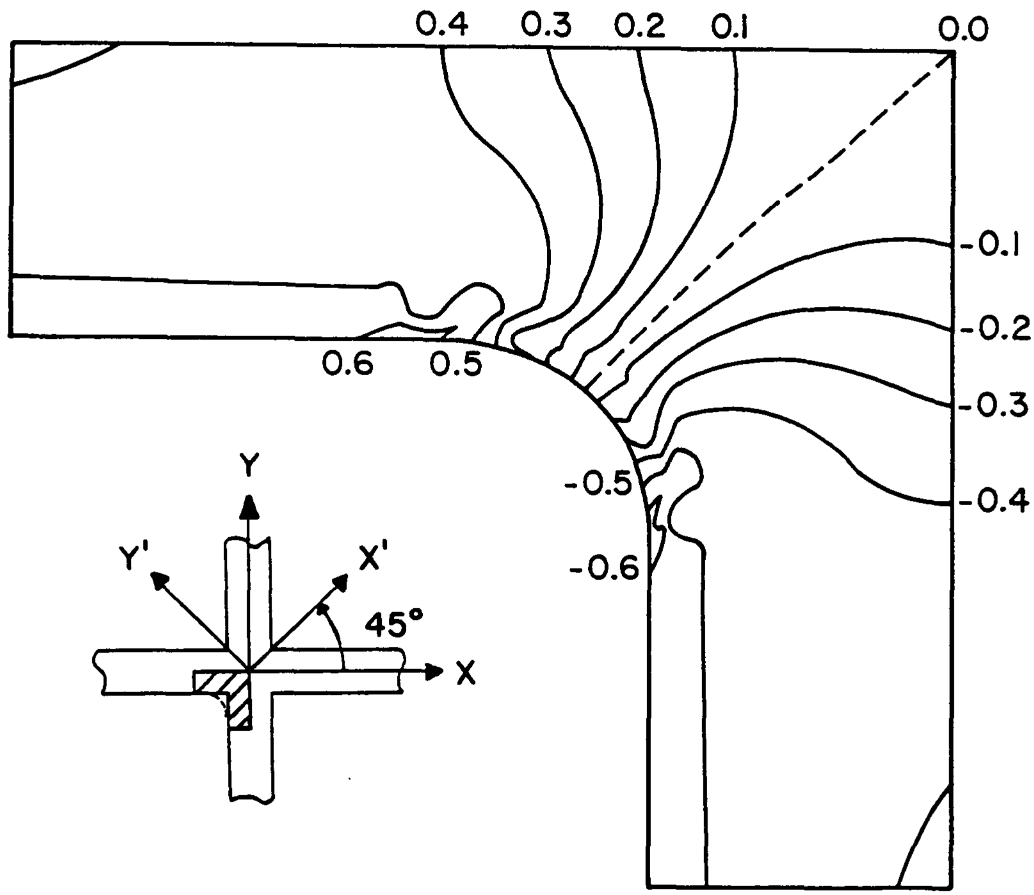

Figure 22. Normalized σ_x' Contours for an Isotropic Cruciform Specimen with 0.33 Inch Corner Radii

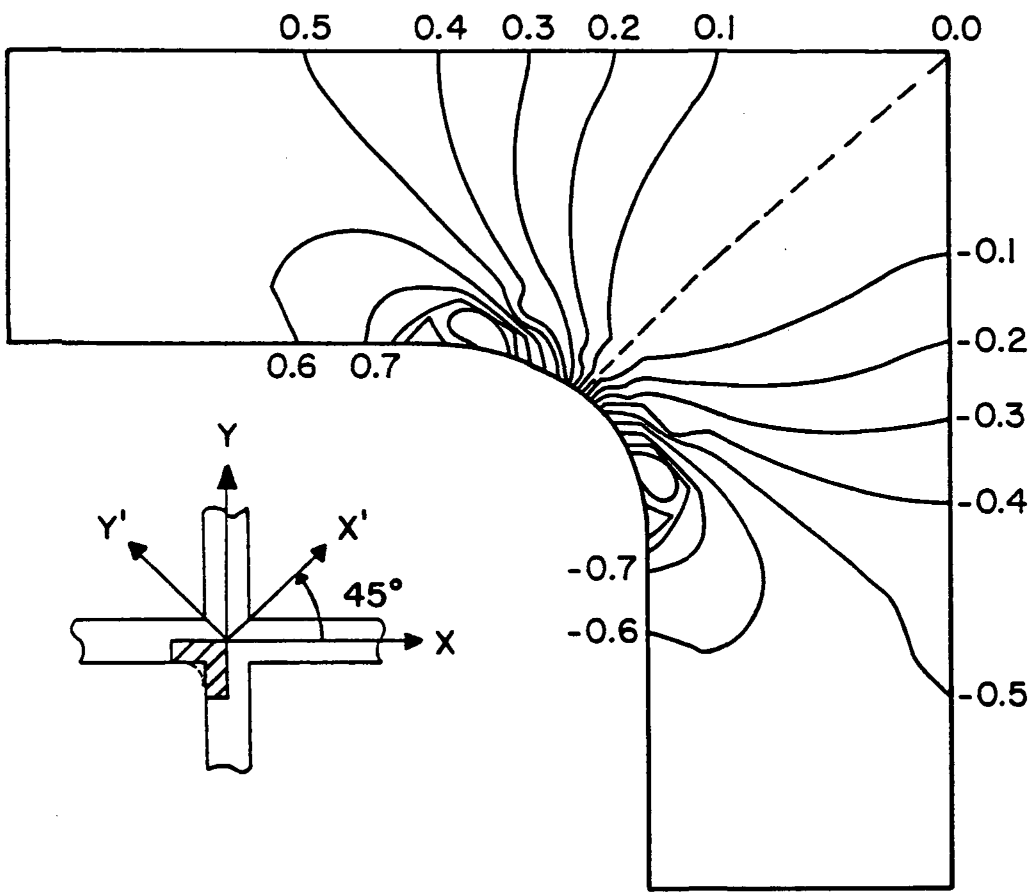

Figure 23. Normalized σ_y' Contours for an Isotropic Cruciform Specimen with 0.33 Inch Corner Radii

$[0/90]_s$ Laminate

Figures 24-26 show the results for the $[0/90]_s$ laminate. As in the isotropic case, there was a region of pure shear in the test section with a value of τ_{xy}'/σ equal to 1.004, and measurment of shear modulus should be very accurate. The severe stress gradients observed with other geometries have been distributed along the arc of the radius, and their effect on the stress state in the center of the test section have been reduced.

$[\pm 45]_s$ Laminate

Figures 27-29 show the results for the $[\pm 45]_s$ laminate with 0.33 inch corner radius. As in the previous cases, a region of pure shear existed in the center of the specimen, with a value of τ_{xy}'/σ equal to 1.021. The applied stress was 2.1 percent higher than the stress in the center of the test section, and measurement of shear stiffness based on the applied stress should be accurate. The radius could be increased slightly to obtain τ_{xy}'/σ equal to 1.0. As observed in the previous two cases, the severe stress gradients have been distributed along the arc of the radius and their effect on the shear stress in the test section was minimal.

These results show that the measurement of shear modulus from specimens of this configuration should be very accurate. Also, the same configuration can be used for isotropic and orthotropic materials as previously shown in Figure 20.

The results from the finite element analysis were again used in the Tsai-Wu failure analysis program. For all three cases, Tsai-Wu failure theory predicted failure of these specimens will initiate at the point where the radius became tangent to the leg of the cruciform.

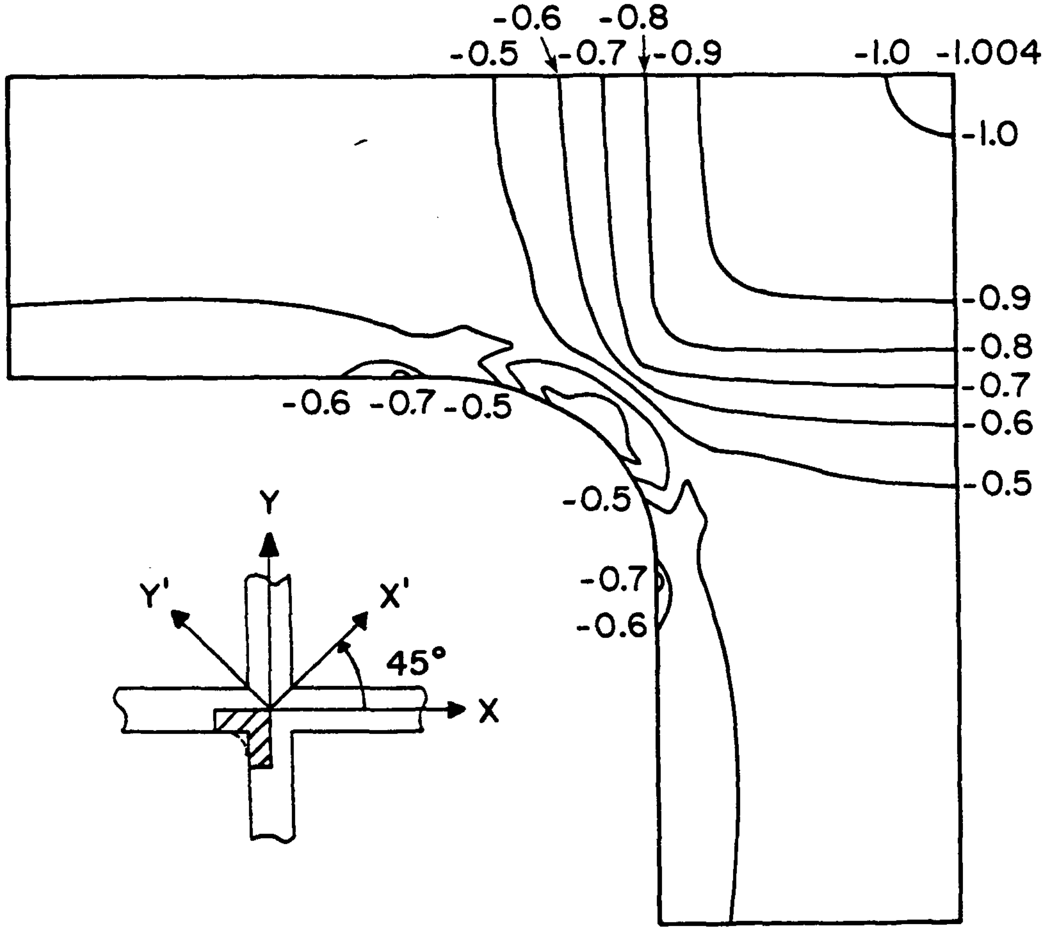

Figure 24. Normalized τ_{xy}' Contours for a $[0/90]_s$ Cruciform Specimen with 0.33 Inch Corner Radius

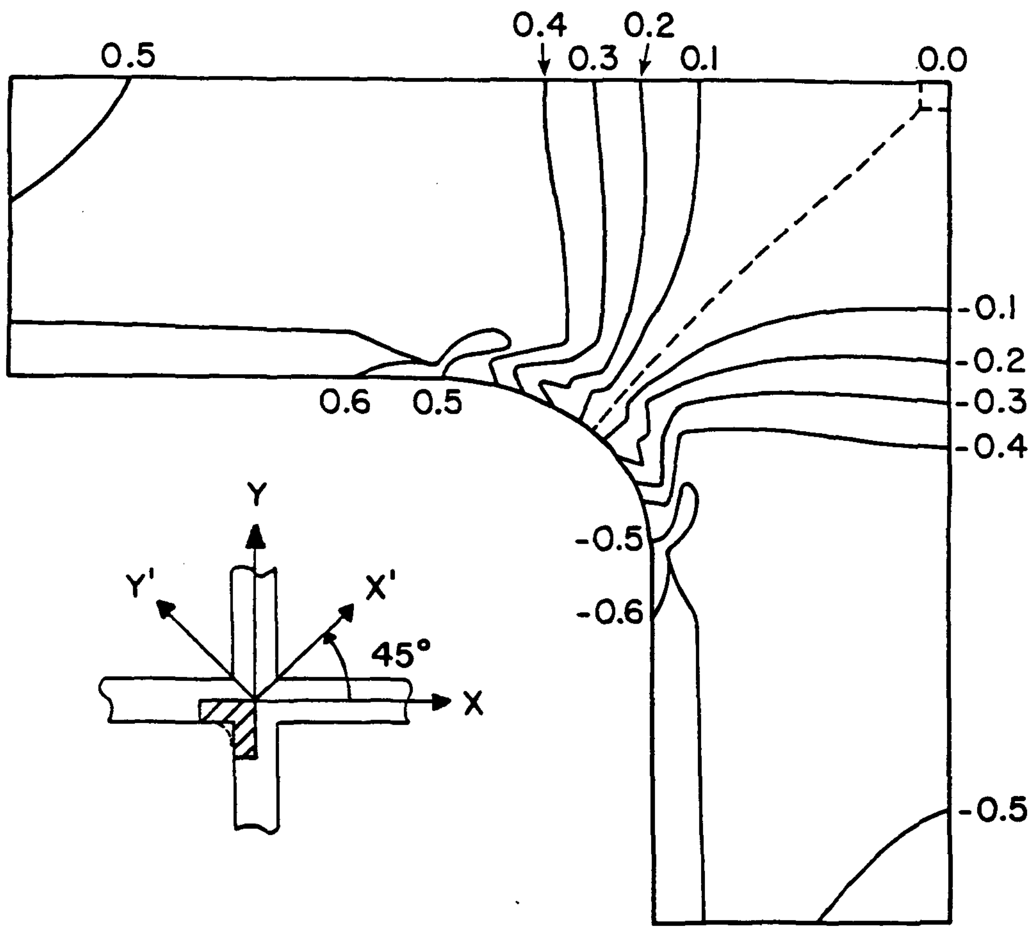

Figure 25. Normalized σ_x' Contours for a $[0/90]_s$ Cruciform Specimen with 0.33 Inch Corner Radius

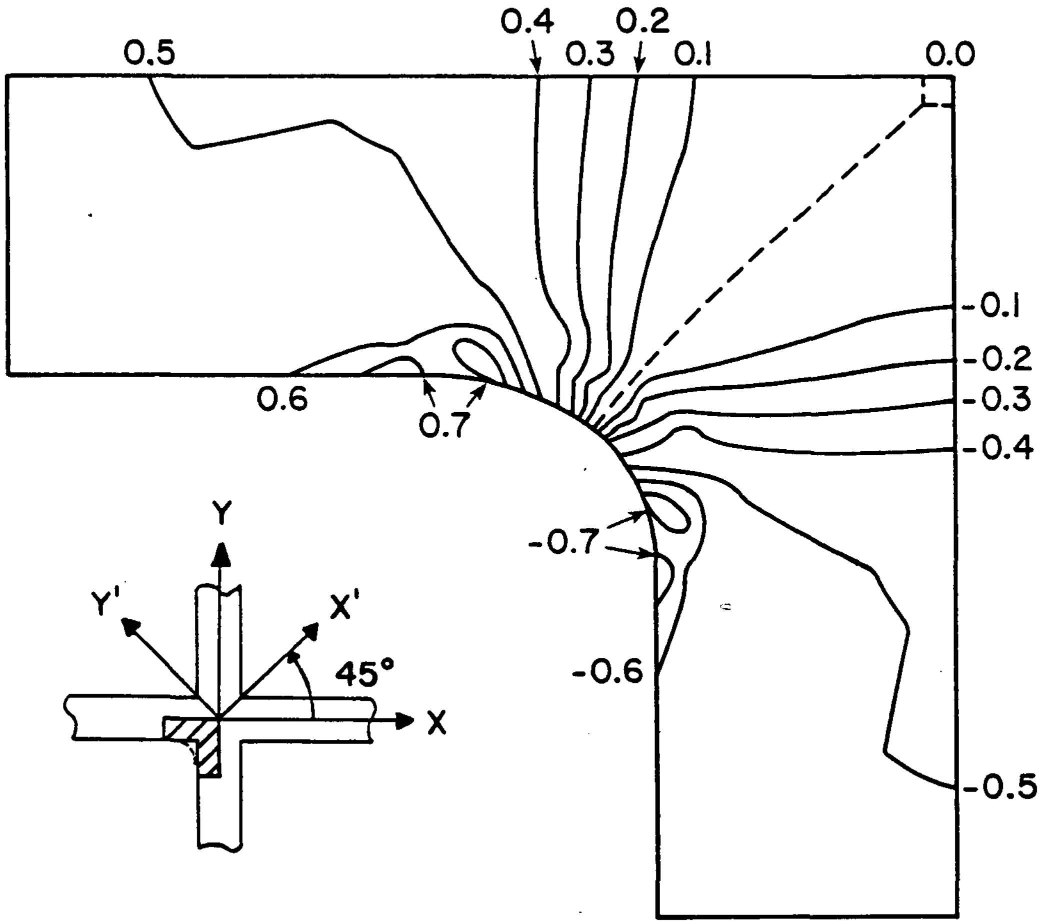

Figure 26. Normalized σ_y' Contours for a $[0/90]_s$ Cruciform Specimen with 0.33 Inch Corner Radius

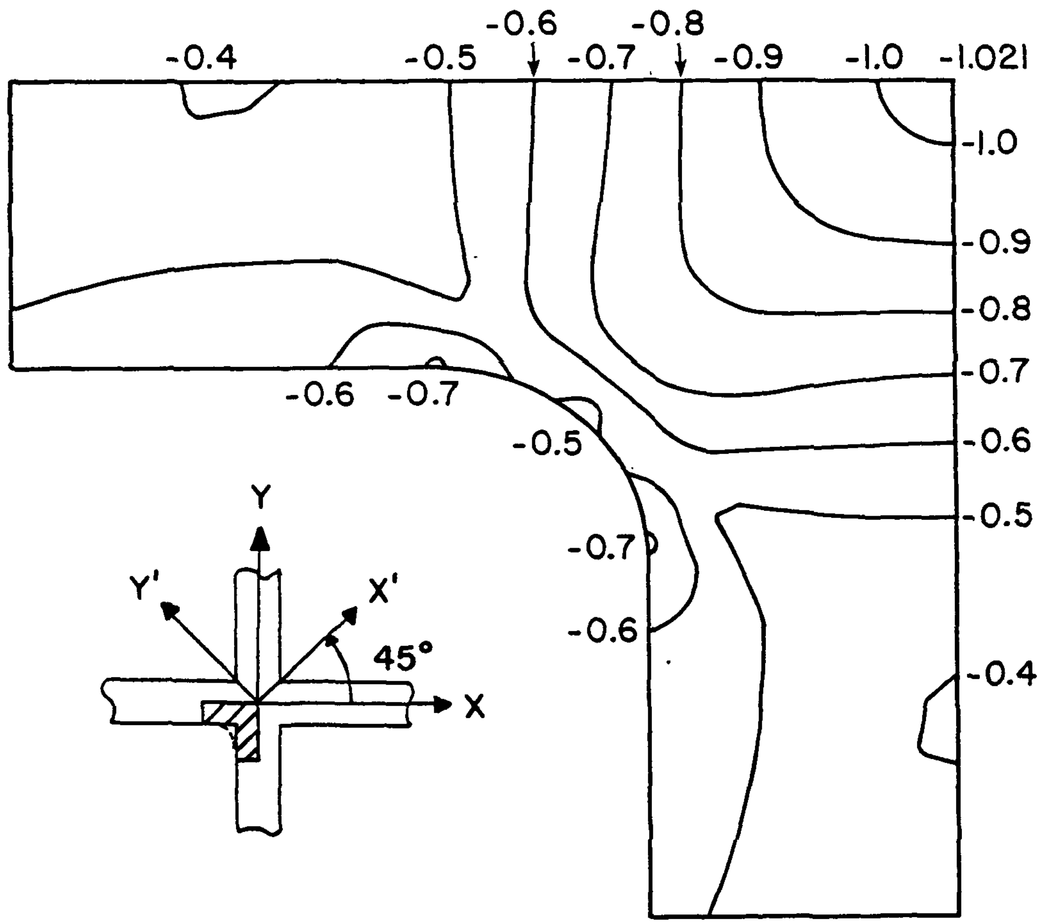

Figure 27. Normalized τ_{xy}' Contours for a $[\pm 45]_s$ Cruciform Specimen with 0.33 Inch Corner Radius

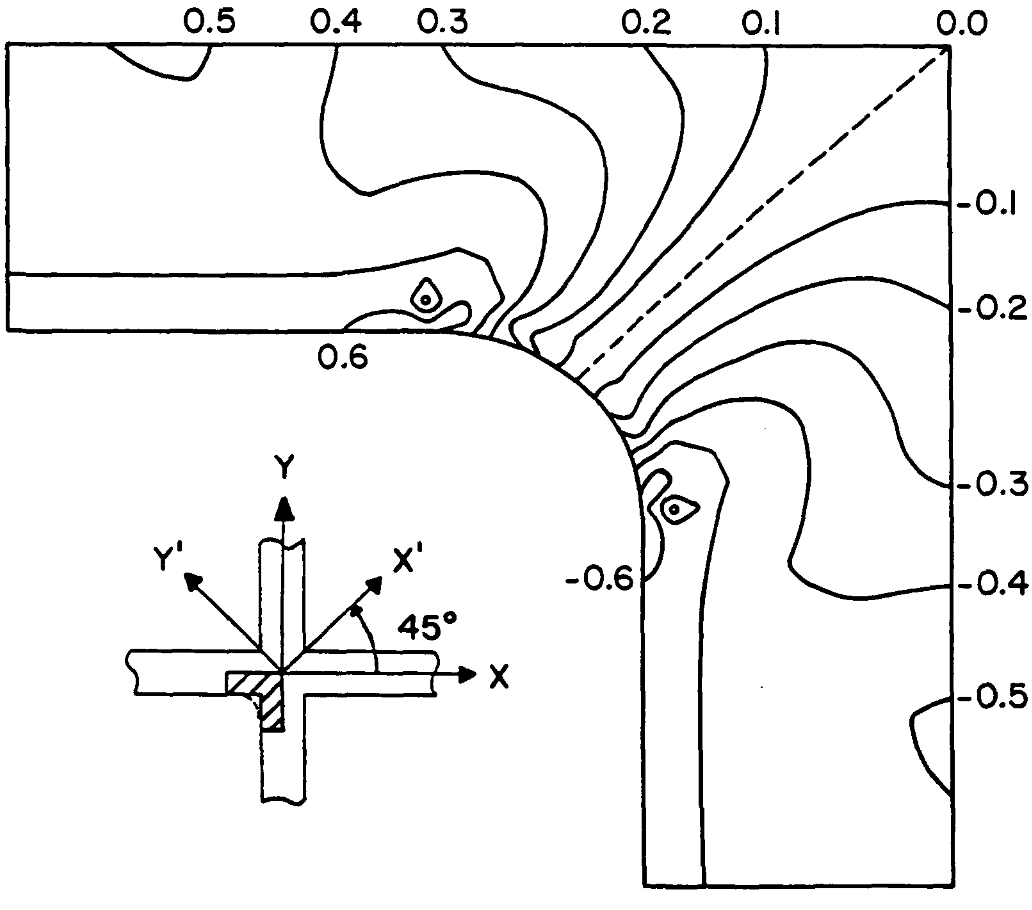

Figure 28. Normalized σ_x' Contours for a $[\pm 45]_s$ Cruciform Specimen with 0.33 Inch Corner Radius

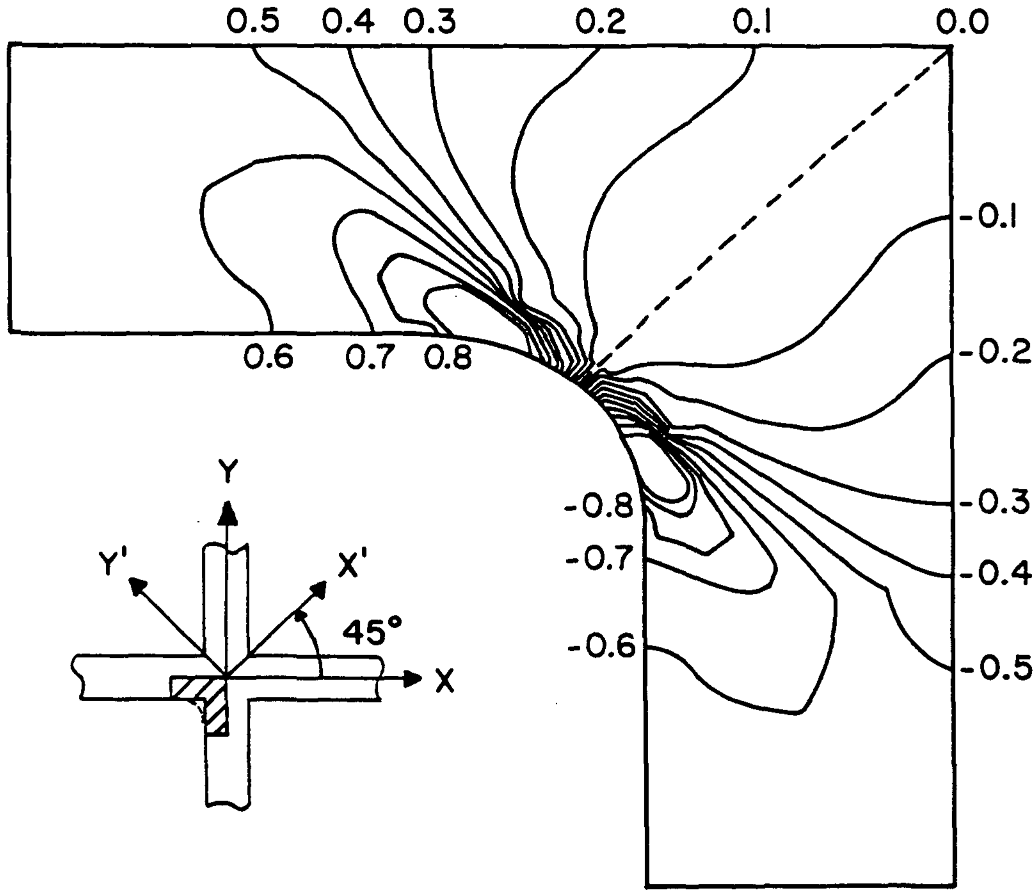

Figure 29. Normalized σ_y' Contours for a $[\pm 45]_s$ Cruciform Specimen with 0.33 Inch Corner Radius

Effect of Pin Loading

The effect of pin loading was also investigated using finite element analysis. By a trial and error process, the length of the legs of the cruciform was determined which gave a uniform stress field in the region between the pin and the test section boundary. The satisfactory length was 2.0 inches from the center of the pin to the edge of the test section.

CHAPTER III

EXPERIMENTAL PROGRAM

An experimental program was conducted to investigate the shear stress-strain behavior of isotropic and composite laminates, and to determine the suitability of the cruciform test method. The initial phase of the program involved fabrication of the cruciform specimens and a test fixture. The final phase involved the experimental shear testing of three laminate configurations: (1) isotropic, (2) $[0/90]_{2s}$ graphite/epoxy, and (3) $[\pm 45]_{2s}$ graphite/epoxy.

Material and Test Specimens

The material used to fabricate the isotropic specimens was commercial 6061 aluminum panels with a thickness of 0.125 inches. The composite specimens were made from eight-ply T300/934 graphite/epoxy panels fabricated at NASA Langley Research Center. The average thickness of these panels was 0.04 inches. An average thickness was used for all stress calculations because all composite specimens were made from the same prepreg. Variation in thickness is due only to small differences in surface finish or fiber volume fraction.

The specimens were cut from the panels at Clemson University. The $[0/90]_{2s}$ and $[\pm 45]_{2s}$ graphite/epoxy specimens were cut from the same panel by orienting the fibers at 0° and 45° to the cutting direction. The necessary pinholes and corner radii were made using diamond hole-saws and carbide drill bits. The corner radii and fixture pinholes in the tabs were precision drilled.

Four specimens of each laminate configuration were made: two with corner radii of 0.344 inches (11/16 inch diameter), and two with sharp corners. Typical cruciform specimens are shown in Figure 30. The length of the legs of the cruciforms was 2.5 inches. Each leg had a 0.375 inch pinhole drilled half an inch from its edge. Micro-Measurement CEA-XX-UR120 rosettes were mounted on front and back of the specimens to measure strain at 0°, 90°, and 45° to the loading direction.

Figure 31 shows the components of an unassembled specimen and a finished specimen ready for testing. For load introduction, aluminum tabs (2.5 x 1.0 x .25 inches) with special guide pinholes were made. These pinholes were drilled at the extreme corners of the tabs and specimens. The specimens and tabs were lightly sanded and then cleaned with methyl-ethyl ketone in preparation for bonding. Dowel pins were inserted in the alignment holes during the tab/specimen bonding process to align the tabs and specimen properly. Tabs were bonded using Hysol EA-9309NA, an industrial strength, room temperature curing adhesive. The bond-line extended from the edge of the tab to approximately half the leg length. This allowed for free displacement of the boundaries of the test section, which more closely simulated the finite element analysis. The tab adhesive was allowed to cure at room temperature seven days under a slight clamp pressure. During the testing process, no debonding between tabs and specimens was observed and this procedure is recommended for similar tests. To insure that the specimen would fit properly into the test fixture and to remove any excess adhesive, the fixture pinholes were reamed 0.001 inch oversize.

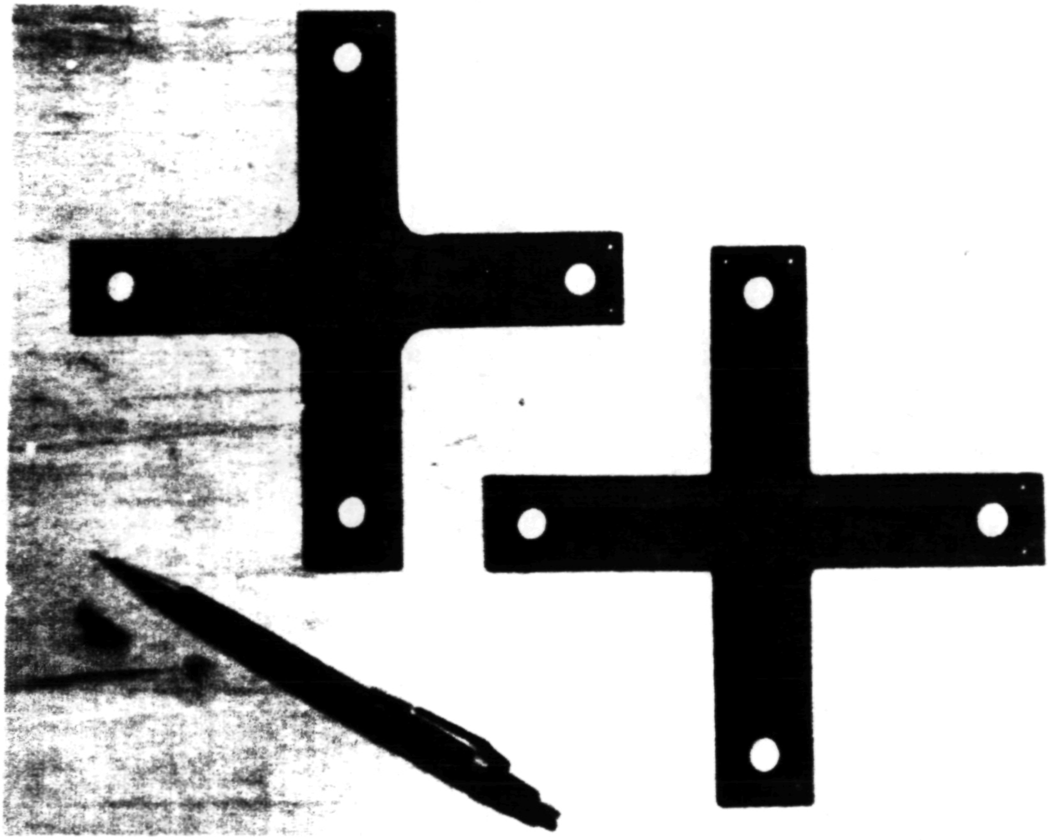

Figure 30. Typical Graphite/Epoxy Cruciform Specimens

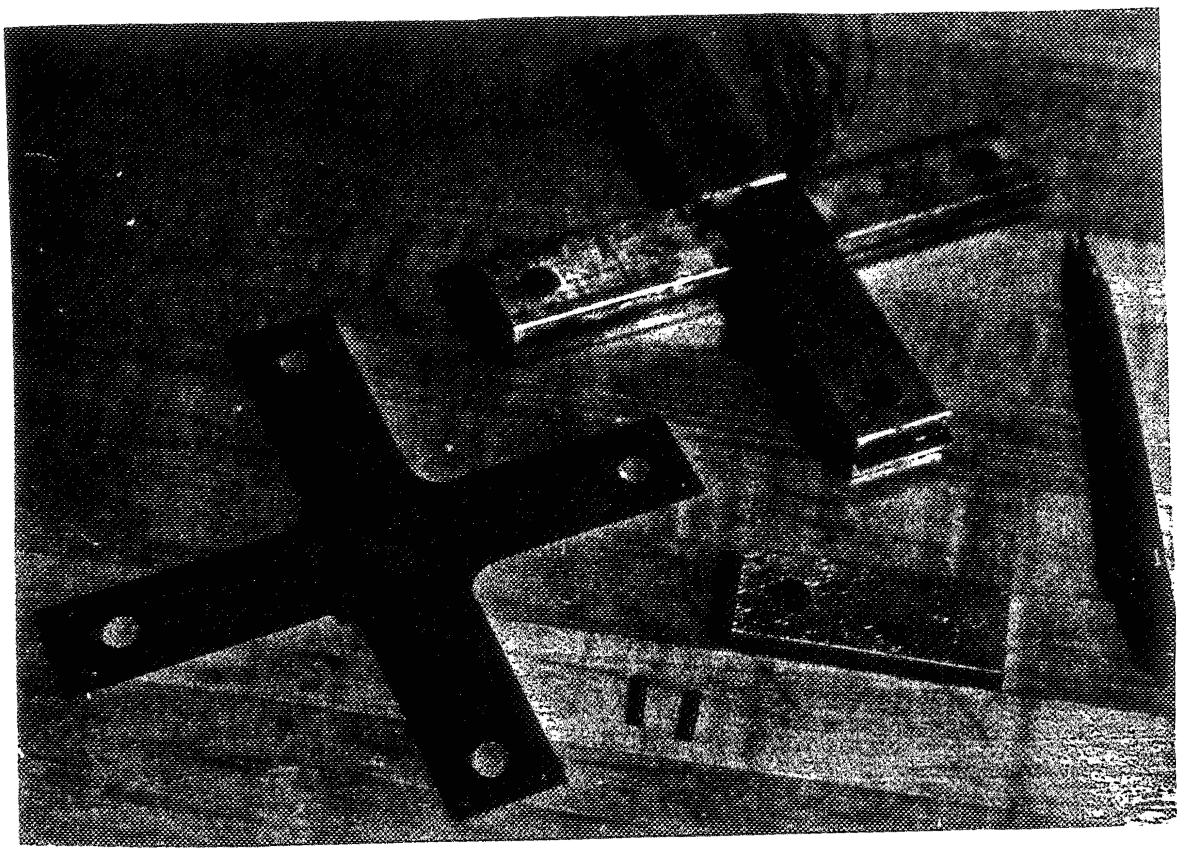

Figure 31. Unassembled and Assembled Cruciform Specimens

Test Fixture

A test fixture made of 17-4 PH stainless steel was fabricated for testing the cruciform specimens. The fixture (Figure 32) was designed so that through kinematics, an equal and opposite pair of biaxial loads could be introduced into the specimen with the application of only an axial load. The fixture had very tight tolerances and was very massive so that deformations in the fixture would be small. The fixture was designed to test specimens with a maximum thickness (including tabs) of 0.75 inches. For thinner specimens, spacers were made to constrain the specimen from buckling in compression. Engineering drawings of the entire test fixture are given in the Appendix.

Because of kinematics of the fixture, an equal and opposite pair of forces can be introduced into the specimen only if displacements are small. Figure 33 shows that for very small displacments, the displacement of Point A is almost equal to that of Point B and the corresponding strains measured in these directions should also be equal. Test data from the aluminum and $[\pm 45]_{2s}$ specimens showed that the strains parallel to the legs of the specimen were equal in magnitude for the entire test. Since the fixture applies only equal and opposite strains, only laminates with $E_x=E_y$ and no shear coupling will give a pure shear state at 45° to the applied load direction (8).

Accurate pin location in the fixture and specimen is very important in relation to the applied tensile and compressive loads. If pin location is inaccurate, the specimen could be loaded in tension (or compression) only, and a pure shear stress state will not result.

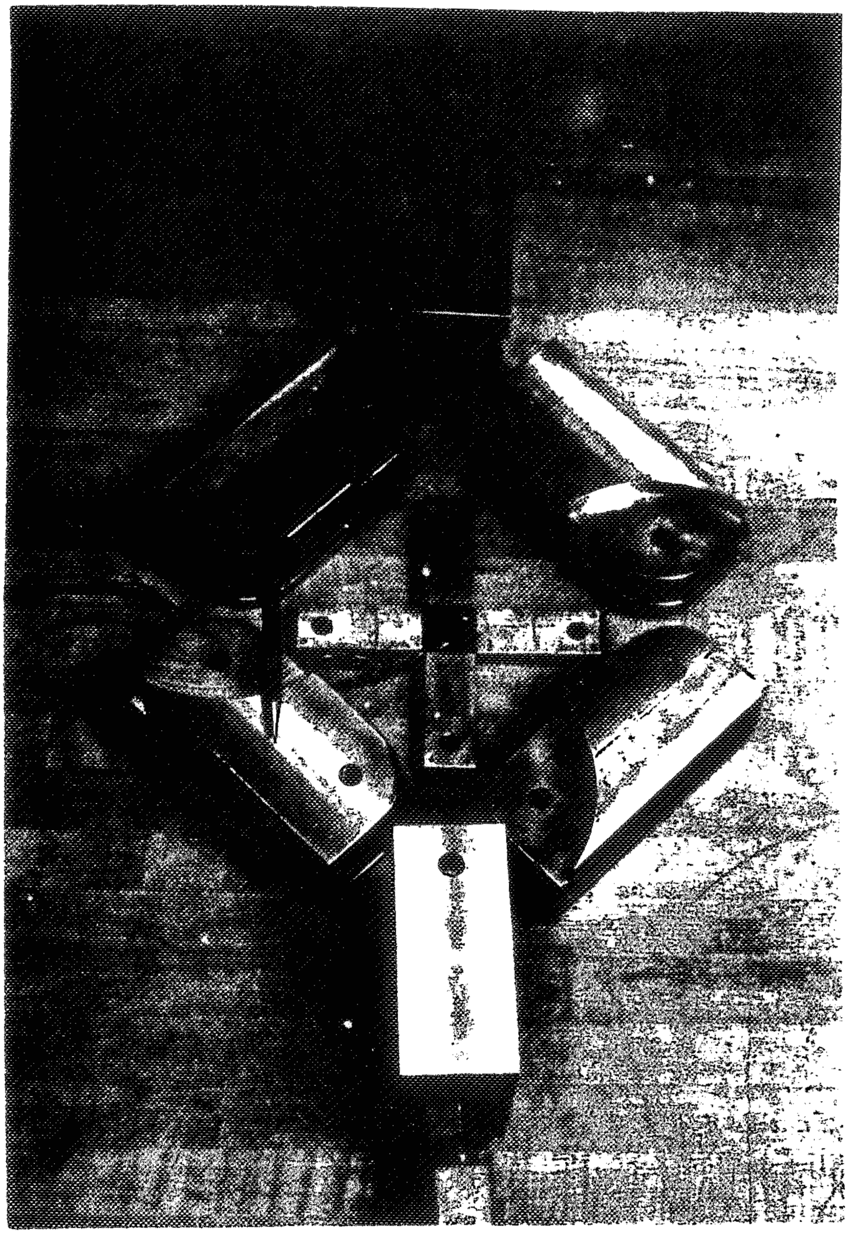

Figure 32. The Unassembled Cruciform Test Fixture and Specimen

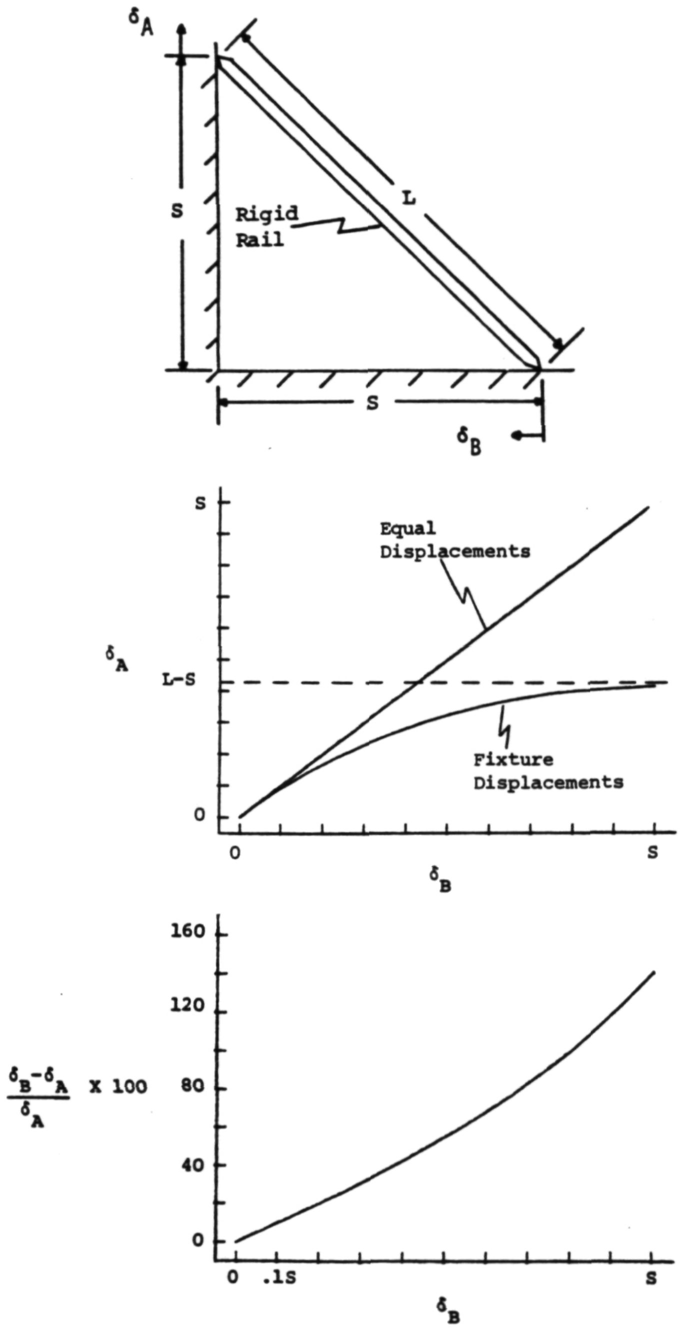

Figure 33. Kinematics of a Rigid Rail

Test Procedure and Equipment

All tests were conducted using a hydraulically actuated, closed loop testing machine. The load was increased linearly with time and a 16-bit digital data acquisition system recorded loads and strains every second. Specimens were loaded to failure or until there was severe yielding. Figure 34 shows the assembled fixture and specimen in the testing machine.

The only problem encountered during the experimental phase was the testing of the thicker aluminum specimens. In this case the 3/8 inch diameter pins bent, but it did not appear to influence the results. This problem can be alleviated by using a larger pin. A pin of 7/16 inch diameter would increase the net cross-sectional area by 36 percent.

Experimental Results

Specimen Performance

Figure 35 shows difference in the shear strain calculated from the opposing strain gage rosettes on a $[\pm45]_{2s}$ laminate. These results were typical of tests on this laminate and the aluminum specimens. The experimental shear strains calculated from the front (γ_f') and back (γ_b') rosettes were within 5 percent of each other. The shear strain, γ_{xy}', was the average of the two gages. This result showed that the fixture and tabs were applying uniform tensile and compressive loads equally through the thickness of the laminates.

The initial test results for the $[0/90]_{2s}$ laminates showed that the laminates were bending out-of-plane, despite the fact that the spacers were used. Figure 36 shows a plot of the strains measured from the compression arm of the rosettes on the opposite faces of the specimen. One gage showed an increase in compressive strain as the load increased, while

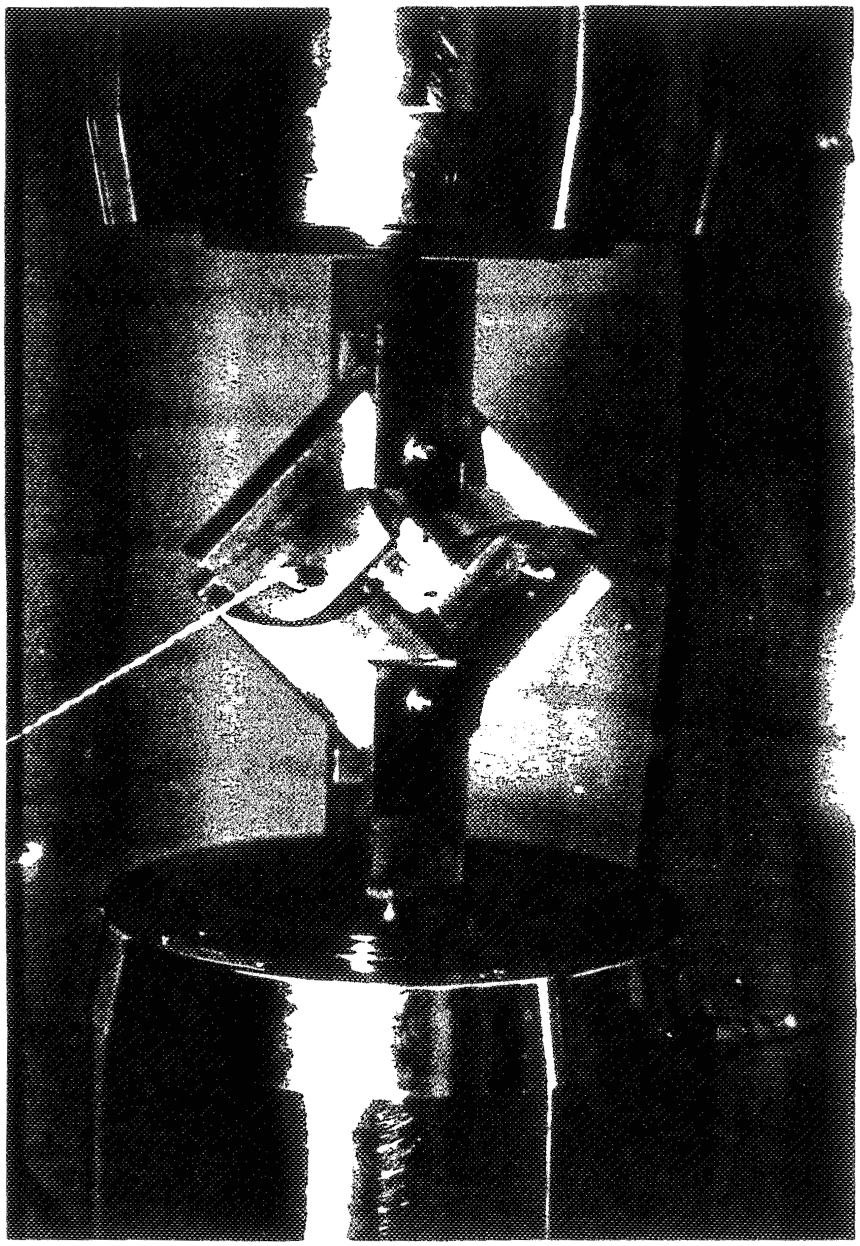

Figure 34. The Assembled Fixture and Specimen in the Testing Machine

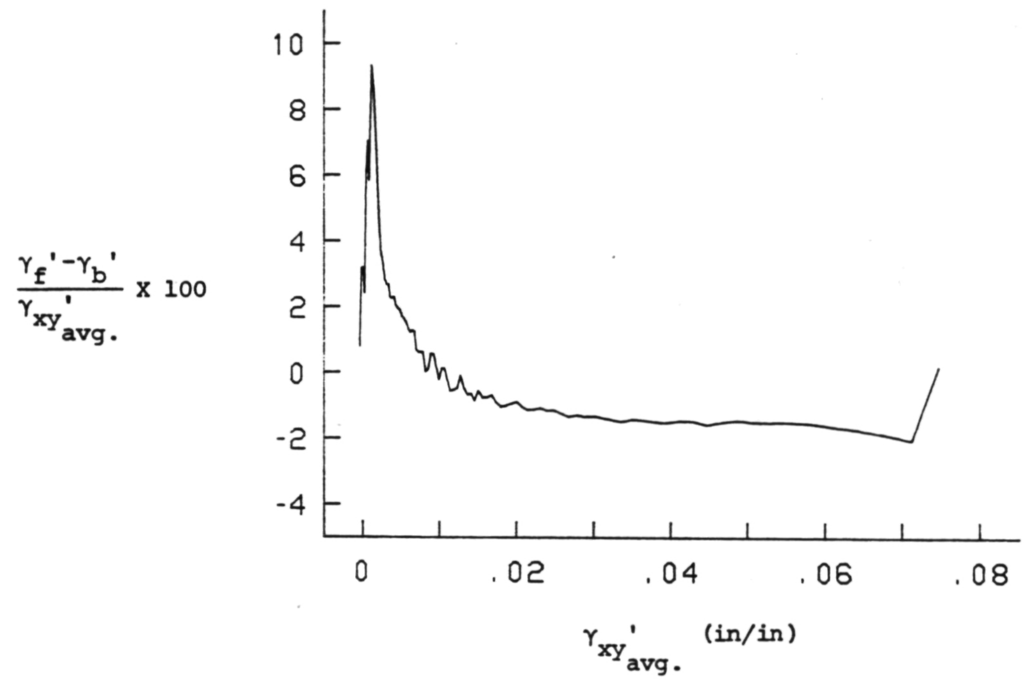

Figure 35. Uniformity of Shear Strain In the Laminates

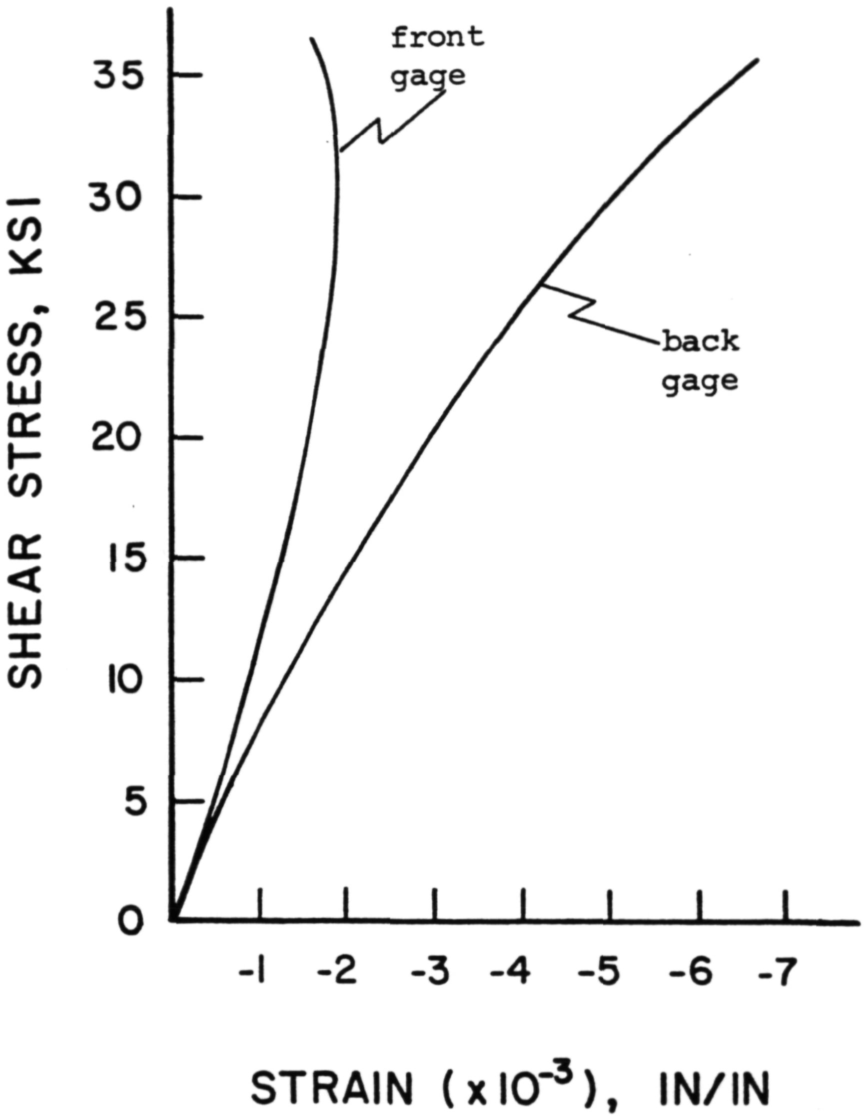

Figure 36. Bending of the $[0/90]_{2s}$ Graphite/Epoxy Laminates

the other showed a decrease, which clearly indicated bending. The aluminum and $[\pm 45]_{2s}$ laminate did bend.

To increase the bending stiffness of these laminates, a set of modified tabs were fabricated. These tabs extended into the original test section of the specimens. A specimen with sharp corners and one with corner radii were tested using the modified tabs. Figure 37 shows a plot of the compressive strains measured from rosettes on opposite faces of the specimen with sharp corners. The strains were colinear until a very high stress level was obtained, but then the strains diverged, which indicated the specimen had buckled. It appeared that the modified tabs would function properly at lower stress levels. However, the results of the test on the specimen with corner radii did not show this. This specimen exhibited the bending behavior shown in Figure 36. From these results, it appeared that alignment for $[0/90]_s$ type laminates was critical.

Figure 38 shows the principle shear strain angle, θ_p, calculated for increasing values of γ_{xy}' for a $[\pm 45]_{2s}$ laminate. These results were typical of tests on this laminate and the aluminum specimens. At very low strains, there was slight variation. As the load increased the principle strain angle approached 45°, the angle required for pure shear strain. This plot confirmed that the fixture was indeed applying equal and opposite loads. As mentioned, the $[0/90]_{2s}$ exhibited out-of-plane deformations and the difference between shear strain calculated from the opposing gages exceeded 10 percent.

Shear Stress-Strain Response

The shear stress-strain curves obtained for the aluminum and the graphite/epoxy laminates with corner radii and sharp corners are shown in Figures 39-41. The initial shear stress-strain response of all

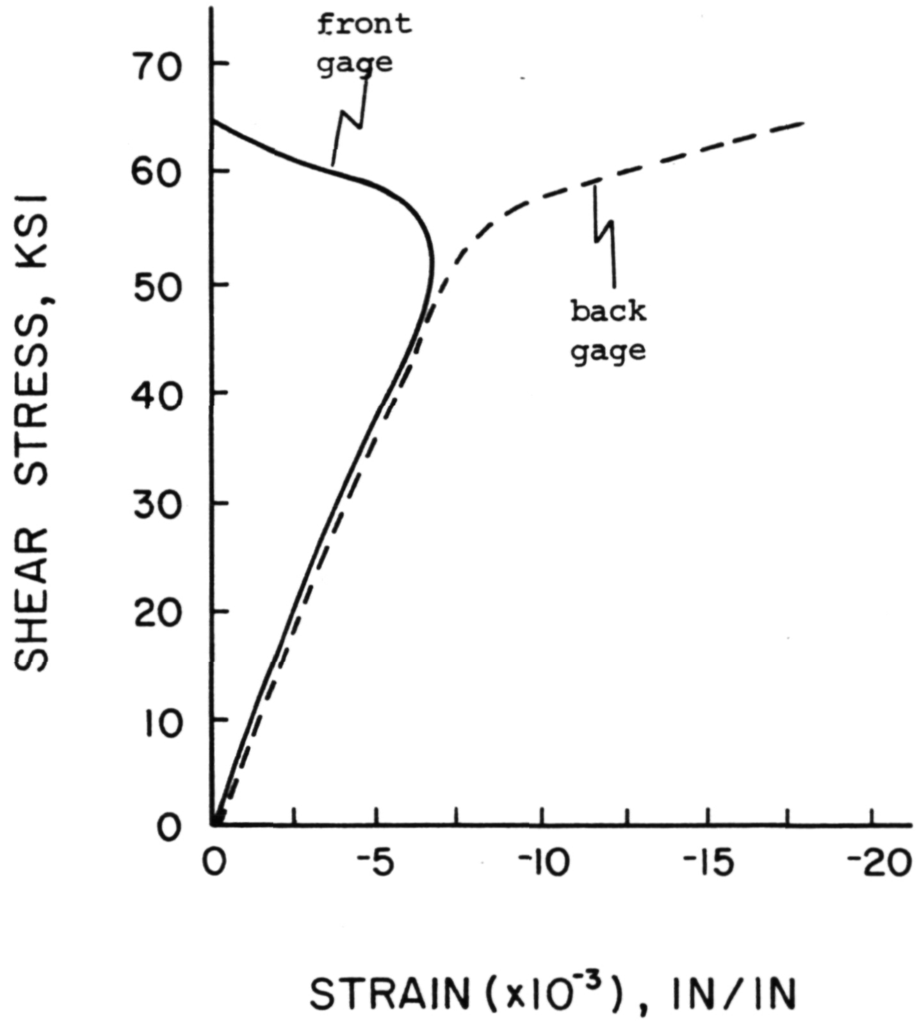

Figure 37. Buckling of the $[0/90]_{2s}$ Laminate with Modified Tabs

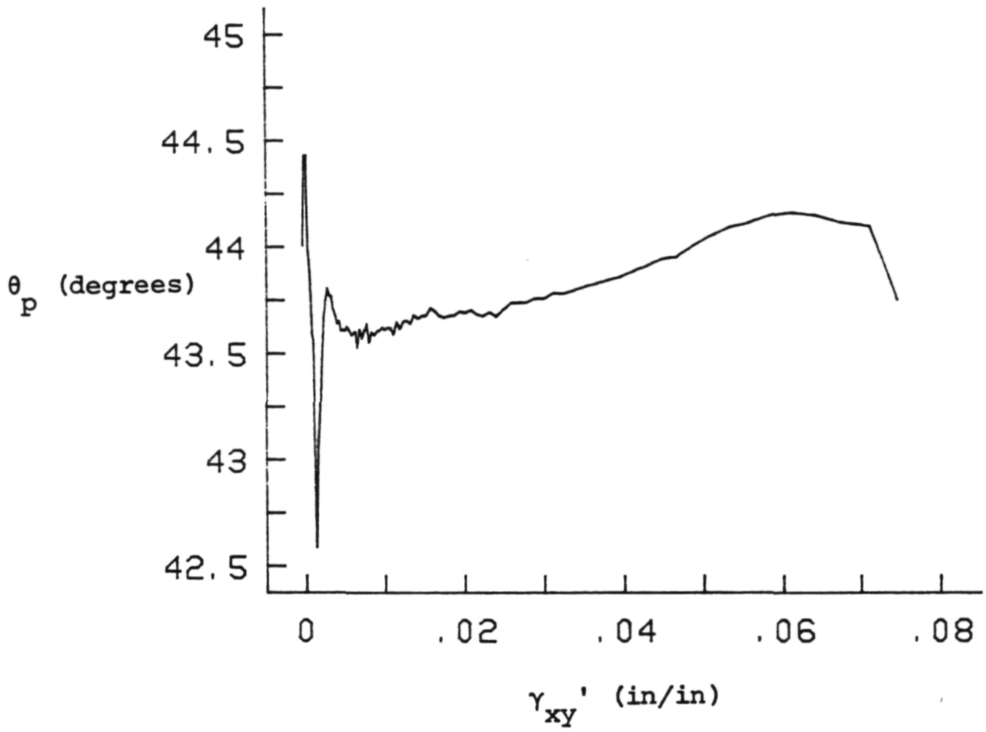

Figure 38. Measured Principal Shear Strain Angle for a Typical Test

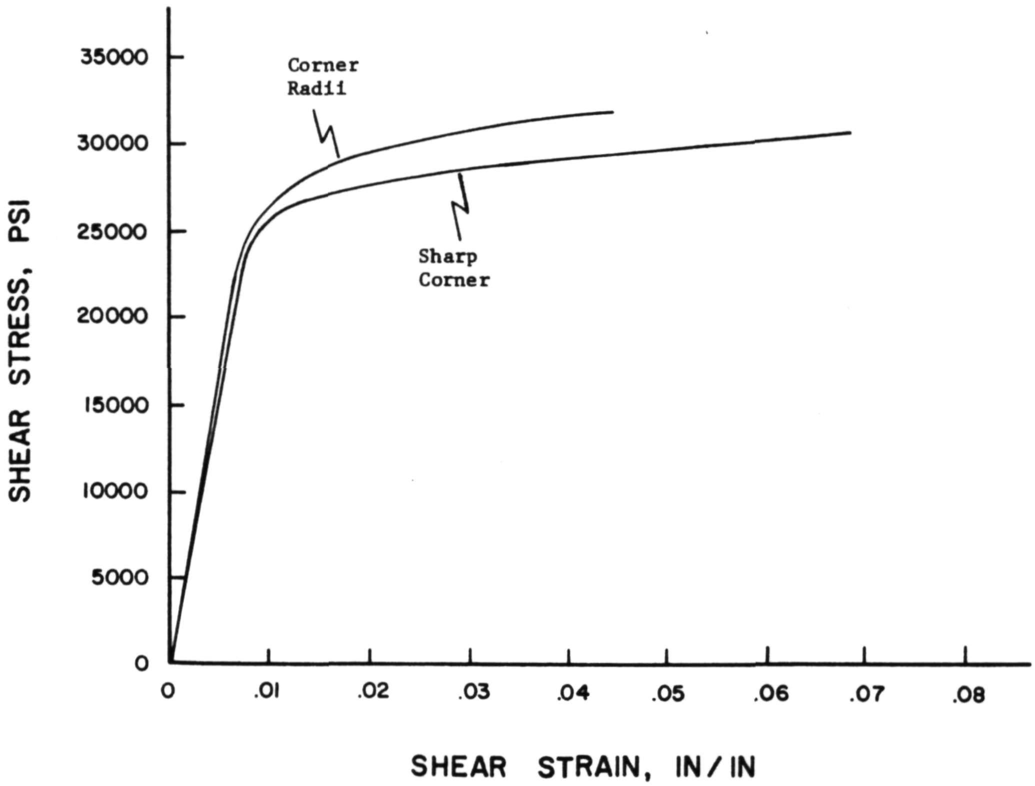

Figure 39. Shear Stress-Strain Response of 6061 Aluminum Specimens

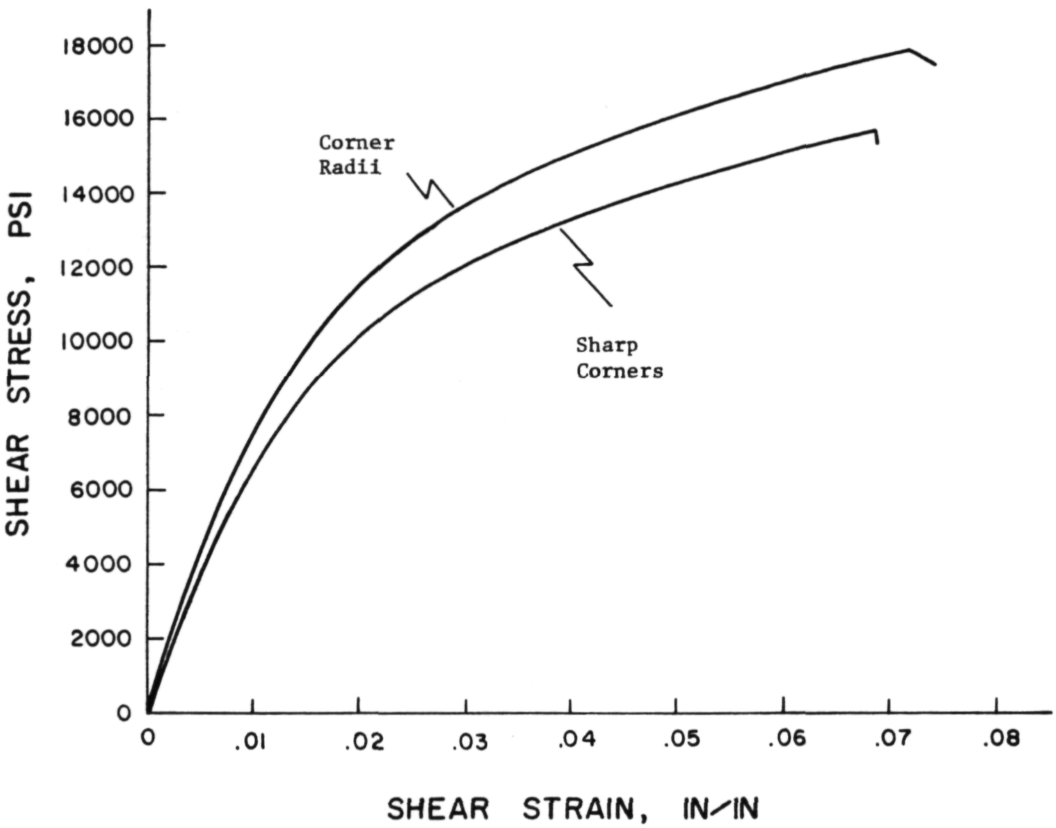

Figure 40. Shear Stress-Strain Response from T300/934 $[\pm 45]_{2s}$ Graphite/Epoxy Specimens

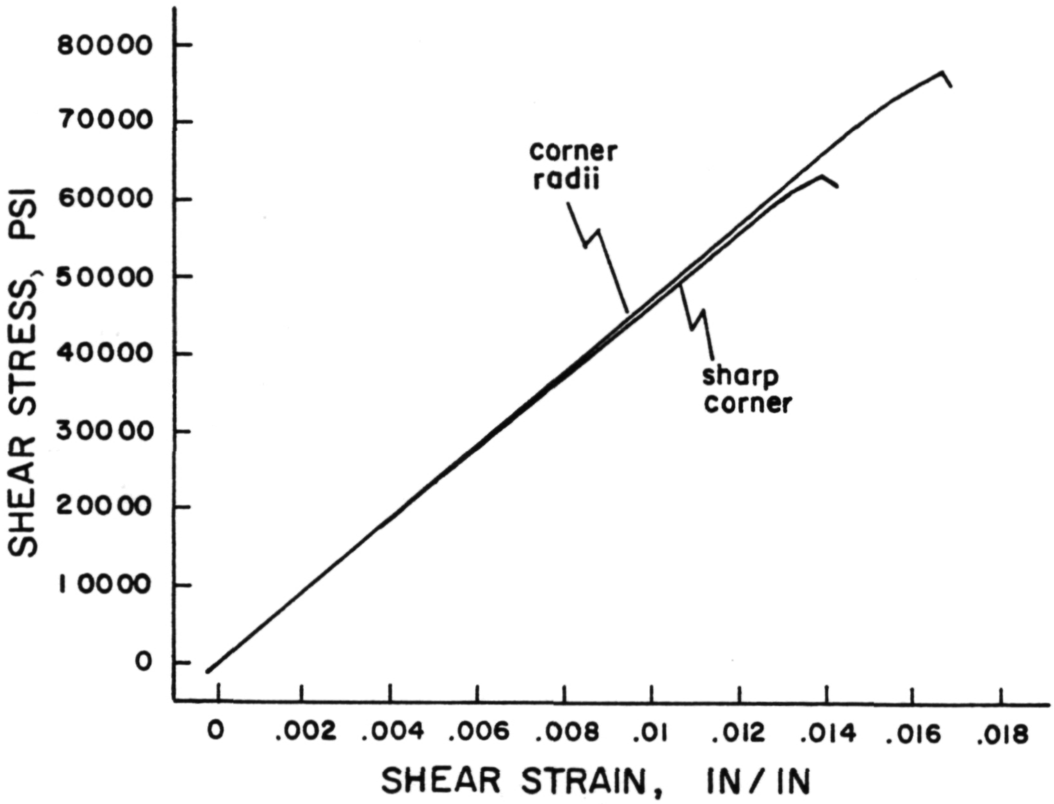

Figure 41. Shear Stress-Strain Response from T300/934 $[0/90]_{2s}$ Graphite/Epoxy Specimens

materials was linear. The shear strain for a particular test was calculated by averaging the shear strain measured from the opposing rosettes of the specimens. The magnitude of the shear stress in the center of the test section was taken to be equal to that of the applied stress. The shear modulus G_{xy}' for each test was determined by performing a linear regression to the initial portion of the stress-strain curve. The shear modulus and strength reported herein for the aluminum and $[\pm 45]_{2s}$ specimens was the average of two tests of each geometry. For these two materials, the difference in shear modulus for any two tests of the same geometry was less than 3 percent. The modulus and strength reported for the $[0/90]_{2s}$ was the results from the specimens with modified tabs.

Isotropic Material

The shear modulus measured for the the aluminum specimen with sharp corners was 3.57 Msi. The modulus measured for the specimen with corner radii was 3.80 Msi, which compares with the value of 3.71 Msi obtained by Walrath and Adams (9) using the Iosipescu method. No failure stress was obtained because the tests were stopped when severe yielding was observed.

$[\pm 45]_{2s}$ Laminate

As previously mentioned, the $[\pm 45]_s$ laminate gives the shear reponse of $[0/90]_s$ laminates (as well as G_{12}, the laminate shear modulus). The measured shear modulus for the the specimen with sharp corners was 0.85 Msi. The shear modulus for the specimen with corner radii was 0.94 Msi. The ultimate stress obtained for the specimen with with sharp corners was 14.66 ksi. The specimen with corner radii reached the higher value of 17.08 ksi.

Failure of both configurations appeared to initiate in the corners regions, as predicted by the Tsai-Wu analysis. For the specimen with sharp corners, there was a narrow strip of delamination of the outer plies that extended diagonally from corner to corner across the test section. Specimens with corner radii failed in a similar manner, except there was a band of delamination across the test section (Figure 42). This band appeared to have initiated at the point where the radii becomes tangent to the legs of the specimen, i.e., the high stress points.

$[0/90]_{2s}$ Laminate

As mentioned, the $[0/90]_s$ laminate gives the shear response of $[\pm45]_s$ type laminates. The shear modulus measured for the specimen with sharp corners was 4.71 Msi. The measured modulus for the specimen with corner radii was 4.84 Msi. An accurate shear strength could not be obtained for either geometry because both exhibited out-of-plane deformations.

The probable cause of the bending was that the laminate was very stiff in the compression direction and alignment between the pins and the specimen was critical. Any slight initial misalignment would result in out-of-plane bending. In the case of the specimen that buckled, it was believed that there was nearly perfect alignment, and the specimen deformed out-of-plane only after the buckling load was reached. The $[\pm45]_{2s}$ laminate did not bend or buckle because of its compliance, i.e., no fibers in the loading directions, and alignment was not as critical. The aluminum specimens did not deform out-of-plane because of greater thickness (0.125 inches). To alleviate bending, it is recommended that the test section be stabilized. A thicker specimen could be used at the expense of a larger test fixture.

Figure 42. Failure of a $[\pm 45]_{2s}$ Laminate with Corner Radii

CHAPTER IV

GENERAL DISCUSSION

A summary of the shear moduli obtained for each specimen is presented in Table I.

Table I. Comparison of Elastic Shear Modulus

Specimen	Experimental G_{xy}' Corner radius (Msi)	Sharp corner (Msi)	Comparison % Diff.	FEM Predicted % Diff.
Aluminum	3.80	3.57	6.05	6.02
$[\pm45]_{2s}$	0.94	0.85	9.57	11.74
$[0/90]_{2s}$	4.84	4.71	2.68	2.06

As shown, the results obtained from the tests correleted very well with the finite element results. Clearly, the shear modulus measured from specimens with sharp corners was lower than the shear modulus measured from specimens with corner radii based on the shear stress being calculated directly from the applied loads. Figure 43 shows the measured modulus values for the aluminum and graphite/epoxy specimens. Data for the $[0/90]_{2s}$ laminate are the values obtained from the results of only one test of each geometry. The data for the aluminum specimen with corner radii correlated well with data reported by other researchers using different methods, as well as handbook values.

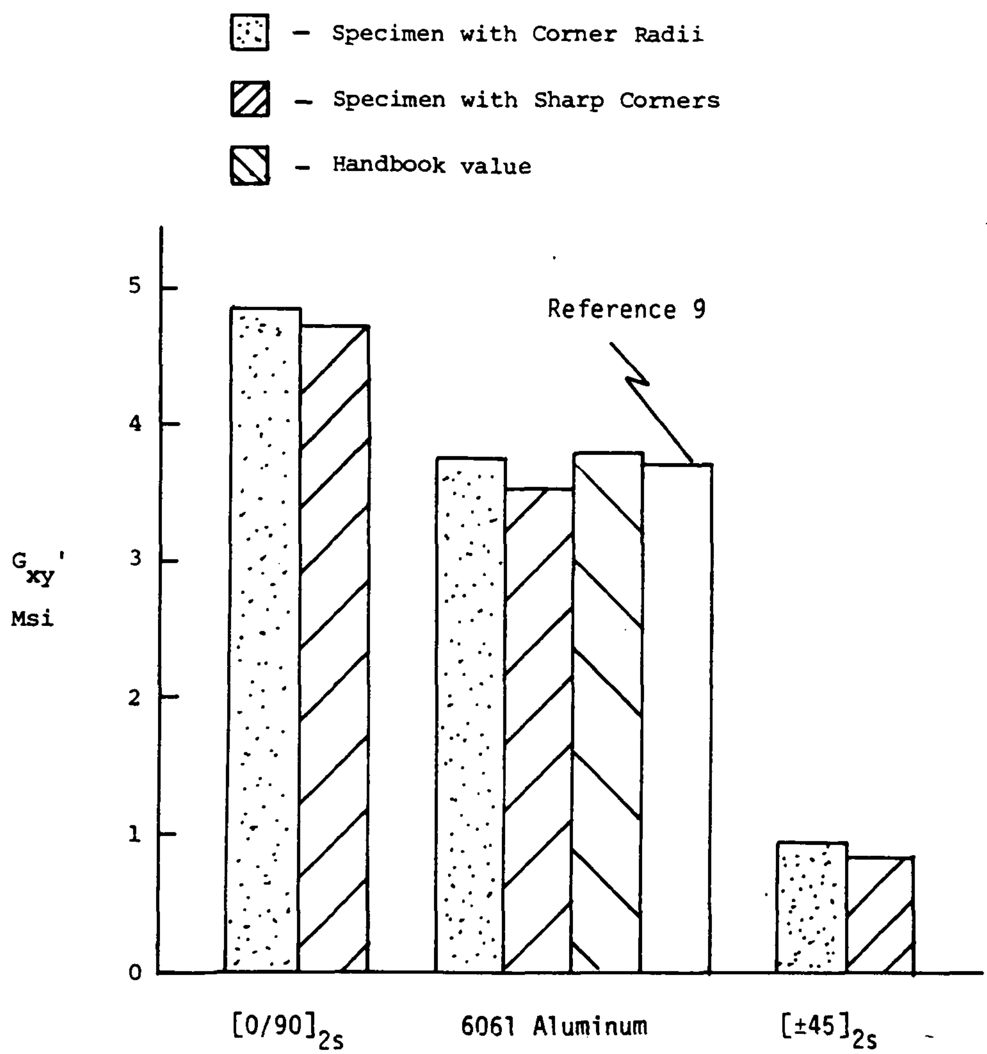

Figure 43. Comparison of Elastic Shear Moduli for 6061 Aluminum and T300/934 Graphite/Epoxy Specimens

A summary of the strength data obtained for the $[\pm 45]_{2s}$ laminate is presented in Table II. No failure data was obtained for the aluminum and $[0/90]_{2s}$ laminate. Failure of the $[\pm 45]_{2s}$ laminate with sharp corners initiated in the corners, as predicted by Tsai-Wu failure theory. For the same laminate with corner radii, Tsai-Wu predicted initial failure would occur at the point of tangency between the radius and the leg of the specimen. This appeared to be the case.

Table II. Ultimate Strength of the $[\pm 45]_{2s}$ Laminates

Configuration	Strength (Ksi)	Failing Strain (in/in)
Sharp Corners		
Specimen #1	13.60	0.058
Specimen #2	15.71	0.069
Average	14.66	0.064
Std. Deviation	1.06	0.006
Corner Radii		
Specimen #1	16.43	0.058
Specimen #2	17.74	0.075
Average	17.09	0.067
Std. Deviation	0.66	0.009

The results from the study show that the cruciform specimen with corner radii was appropriate for determining at least shear stiffness of composite materials. It was shown by finite element analysis that the specimen with sharp corners would yield a lower shear modulus if the magnitude of the stress in the center of the test section was taken to be equal to the applied stress. This was confirmed by the experimental data. The finite element results obtained by this investigation also confirmed work by other researchers studying the same method.

The data from experiments confirmed that the kinematic fixture was applying equal and opposite forces into the specimens. This type of loading restricted shear testing to the class of laminates with $E_x = E_y$ and no shear coupling. Other laminates can be tested, in a kinematic type fixture, but a combined stress state will result. This same specimen geometry can also be used in testing machines that apply biaxial loads that are not equal and opposite in magnitude and a larger class of laminates (with no shear coupling) will have a pure shear stress state at 45° to the applied loads.

The method of bonding the tabs with alignment pinholes to the specimen was a very easy method for assembling the specimens. As previously mentioned, this method is recommended for similar tests.

CHAPTER V

CONCLUSIONS

The results of an experimental and analytical investigation of a biaxial tension/compression test for determining the shear properties of composite materials were reported. The effect of specimen geometry on the stress state of the cruciform specimen was studied using finite element analysis. An optimized specimen geometry was determined. An experimental program was conducted to verify the method. A test fixture was designed to introduce an equal and opposite pair of forces into a cruciform specimen. Aluminum and composite specimens were tested.

The results from the experiments correlated well with the finite element results. The results of finite element analysis and experimental tests lead to the following conclusions:

1. The optimized specimen develops a uniform pure shear stress state over a large region of the test section which results in accurate determination of shear stress-strain response of composite laminates, excluding shear strength.

2. The optimized specimen can be used for isotropic and orthotropic laminates.

3. The optimized specimen requires a small amount of material and is easy to fabricate.

4. The kinematic fixture introduces equal and opposite loads into the specimen and can be used in a universal testing machine.

5. Further revisions to the specimen geometry are necessary if the method is to give shear strength data.

APPENDIX

Engineering Drawings of the Test Fixture

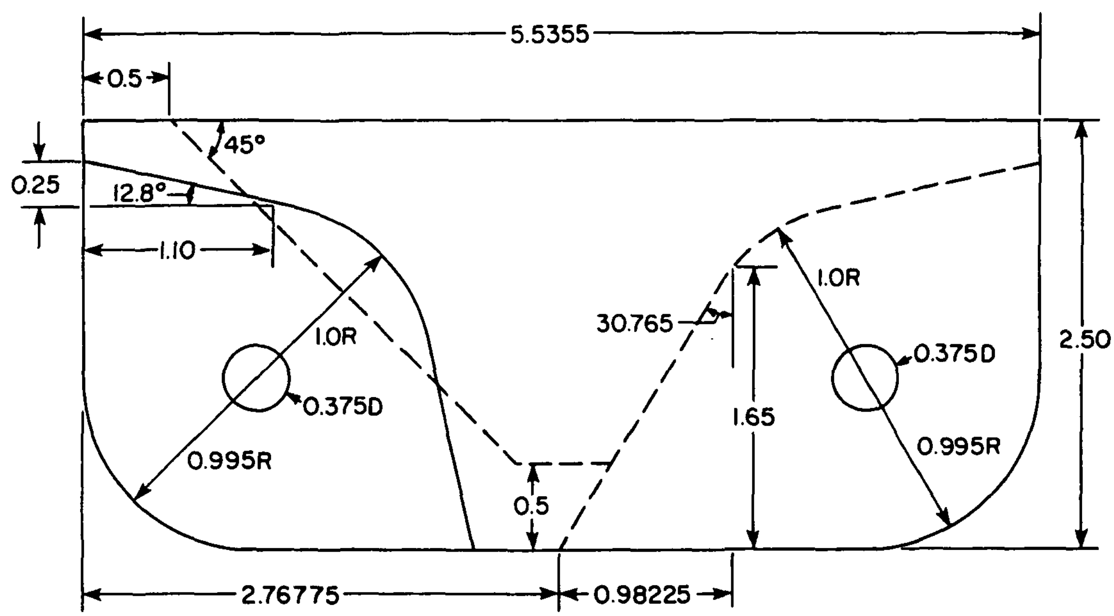

Figure A-1. Rigid Rail of the Test Fixture (Top View)

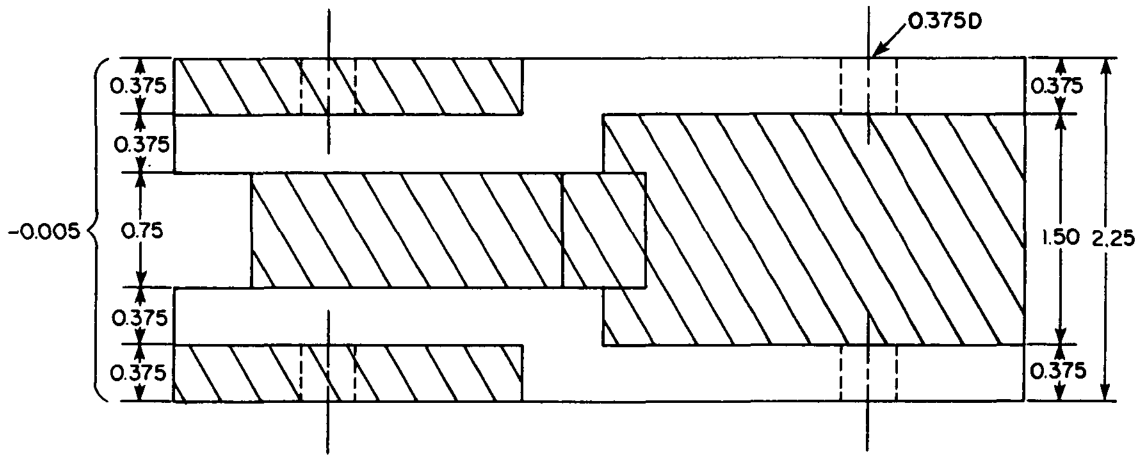

Figure A-2. Cross-Section View of the Rigid Rail

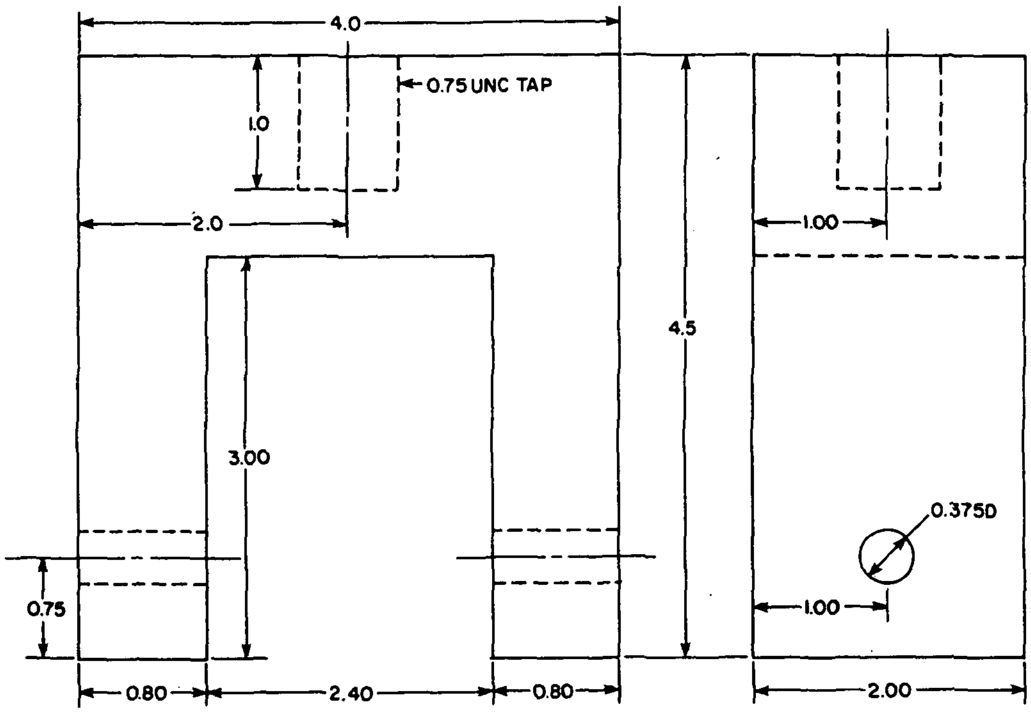

Figure A-3. Load Introduction Clevice

REFERENCES

1. Lee, S., and Munro, M., "In-plane Shear Properties of Graphite Fibre/Epoxy Composites for Aerospace Applications: Evaluation of Test Methods by the Decision Analysis Technique," Aeronautical Note NAE-AN-22, University of Ottawa, Ottawa, Canada, October, 1984.

2. Pindera, M., Choksi, G., Hidde, J. S., and Herakovich, C. T., "A Methodology for Accurate Shear Characterization of Unidirectional Composites," Journal of Composite Materials, Vol. 21, December, 1987, pp.1164-1184.

3. Bergner, H. W., Davis, J. G., and Herakovich, C. T., "Analysis of Shear Test Methods for Composite Laminates," Interime Report Number 6, VPI-E-77-14, NASA Grant 47-004-129, Virginia Polytechnic and State University, Blacksburg, Va., April, 1977; also NASA CR-152704.

4. Duggan, M. F., McGrath, J. T., and Murphy, M. A., "Shear Testing of Composite Materials by a Simple Combined-Loading Technique," AIAA, 1978.

5. Monch, E., and Galster, D., "A Method for Producing a Defined Uniform Biaxial Tensile Stress Field," British Journal of Applied Physics, Vol. 14, 1963, p. 810.

6. Cridland, L. and Wood, W. G., "A Hydrostatic Tension Test of a Brittle Material," Internation Journal of Fracture Mechanics, Vol. 4, Nr. 3, September, 1968, p. 277.

7. Petit, P. H., "A Simplified Method for Determining the In-plane Shear Stress-Strain Response of Unidirectional Composites," Composite Materials: Testing and Design, ASTM STP 460, 1969, p. 83.

8. Jones, Robert M., Mechanics of Composite Materials, Hemisphere Publishing Company, New York, 1975.

9. Walrath, D. E., and Adams, D. F., "Verification and Application of the Iosipescu Shear Test Method," Technical Report, NASA-Langley Research Center, Hampton, Virginia, Grant No. NAG-1-272, June, 1984.